

**ASPECTS OF THE FILAMENT ACTIVITY WITHIN THE  
BENGUELA UPWELLING SYSTEM**

P.L. STOCKTON

Thesis presented in partial fulfillment for the degree of

Master of Arts

AT THE UNIVERSITY OF STELLENBOSCH.

25 November 1988.



Promoter : Dr J.R.E Lutjeharms, EMA, CSIR, Stellenbosch.  
Examiners: Dr W.S. Barnard, Department of Geography, University of Stellenbosch.  
Miss J. Olivier, Department of Geography, University of Stellenbosch.

**DECLARATION**

**I the undersigned declare that the work contained in this thesis is my own original work and has not been submitted in its entirety or in part for a degree at any other university.**

28 November 1988

## AKNOWLEDGEMENTS

At this stage I would like to express my sincere appreciation to those who have assisted and supported me during this research.

**Prof. W. Barnard** acted as Project Leader of the research.

**Department of Geography, University of Stellenbosch.** My colleagues, who generously allowed me to monopolise a microcomputer over the period of this project. They also provided the encouragement and academic stimulation required for effective research.

**Miss B.B. Haldenwang** was always ready to give advice and allow the use of her mapping equipment.

**Dr J.R.E. Lutjeharms** from EMA, CSIR, Stellenbosch, for his invaluable guidance advice and for acting as an example of how research of this nature should be done. Dr Lutjeharms co-authored the majority of the papers and publications produced during the research towards this degree.

**Miss J. Olivier** was first author for one of the papers arising from the research as well as acting as examiner of the final thesis.

**Mrs B. Stockton** gave valuable criticism with regard to the correct language usage.

**Mrs J. Stockton**, my wife, for her unwavering support.

**SADCO Database** of the CSIR made the sea surface temperature and wind data available for use in Chapter 4.

**Sea Weed Research Unit** at the University of Cape Town supplied the undersea temperatures for Betty's Bay, used in Chapter 3.

**Mr H. Valentine** EMA, CSIR, Stellenbosch, who acted as curator of the satellite imagery which was fundamental to this study.

The last word goes to my sponsors. The **CSIR** are thanked most sincerely for the generous funding given to this endeavour. Without their financial and material assistance this thesis would not have been possible.

**LIST OF FIGURES.**

	PAGE
<b>FIGURE 1.1</b> The locations of the major upwelling zones of the world ;  (1) Benguela Upwelling system; (2) Chile and Peruvian Upwelling area; (3) Northwestern Australian Upwelling zone; (4) North African Upwelling regime; (5) Californian Upwelling system.	1
<b>FIGURE 1.2</b> The study area with the locations of the key places and the ocean bottom features mentioned in the text. The ocean floor contours show the depth from the sea surface in metres.	2
<b>FIGURE 1.3</b> A schematic diagram of the upwelling process as found off the western margins of most major landmasses in the southern hemisphere. (a) Indicates a theoretical inactive phase where there is no longshore wind. The isotherms are horizontal. (b) With the onset of a longshore wind an atmospheric Ekman spiral results in the wind stress applied to the water surface being slightly offshore. (c) The spiral continues below the surface resulting in the mean mass transport of the water mass being offshore (1). This is compensated for by a return flow (2) at deeper levels, forcing the cold water to the surface along the coastline.	3
<b>FIGURE 1.4</b> Geographic distribution of identifiably distinct upwelling cells in the South-East Atlantic Ocean. Each dot represents the centre of an upwelling event observed over a period of 156 weeks. (Lutjeharms and Meeuwis, 1987)	4
<b>FIGURE 2.1</b> Thermal infrared satellite image of the South East Atlantic Upwelling system, showing detail of the upwelling front on 26 May 1986. Mesoscale features apparent are the deep sea frontal filaments (A), and the cape filaments (B).	12
<b>FIGURE 2.2</b> The seasonal location of the upwelling core along the west coast of southern Africa (dark shading) and the amorphous, active frontal zone (lighter shade) for 1978, 1979 and 1982. The Meteosat satellite for this area was not operational during 1980 and 1981.	13

- FIGURE 2.3** The seasonal location of the upwelling core along the west coast of southern Africa (dark shading) and the amorphous, active frontal zone (lighter shade) for 1983, 1984 and 1985. 14
- FIGURE 3.1** : Daily wind run diagrams for the 14h00 wind as recorded at Lüderitz during 1982. The stick diagrams show filament extent for each day on which it could be measured. Each day is represented by a dot or stick, starting with the first day of the month at the bottom, progressing to the last day at the top. A dot shows the lack of data for any given day. 21
- FIGURE 3.2** : Visual waveband image of the west coast of southern Africa of 5 July 1982. The extensive dust-plume resulting from a 30 knot berg wind can be clearly seen being transported out to sea. 22
- FIGURE 3.3** : The daily filament extent is given for each day on which it could be measured for 1982 and 1984. The ten day wind stick vector diagrams for the winds blowing at  $10^{\circ}\text{E} \times 25^{\circ}\text{S}$  during 1982 and 1984. The sticks indicate the resultant direction from which the wind was blowing. 25
- FIGURE 3.4** : Thermal infrared image of the west coast of southern Africa of 5 July 1982. The lighter grey path on the image shows the cold filament as it streams into the South-East Atlantic. The box shows the area chosen for the schematic representation of the anticyclonic vorticies which the filament path suggests are possibly active there. 26
- FIGURE 3.5** : Weekly sea surface temperature and wind patterns off the coast of South West Africa during July 1982. The isobaths are given in metres and the sea surface isotherms in degrees Celsius. 28
- FIGURE 4.1** The location of the study area. The mountains are lightly shaded for altitudes in excess of 600 metres. 34
- FIGURE 4.2** The percentage of the extracted sample where filaments were seen off the individual headlands and when they occurred off all three headlands simultaneously. 39

**FIGURE 4.3** The percentage of upwelling occurring for each month in Walker Bay during the years 1978, 1979 and 1982 to 1985.

40

**FIGURE 4.4** A well mixed water body over the Agulhas Bank for 26 September 1986. The thermal infrared image is from the NOAA-9 satellite. The lighter shades indicate lower sea surface temperatures. This sea surface temperature pattern is typical of the winter regime.

41

**FIGURE 4.5** Characteristic upwelling mode as it appears along Southern Africa's south western Cape Coast for 12 December 1986. Typical summer cape induced filaments are being advected from Cape Agulhas, Cape Hangklip, Cape Point.

42

**FIGURE 4.6** Image of a typical summer upwelling pattern between Cape Point and Cape Agulhas for 6 February 1986. Although the upwelling is apparently influenced by the capes, it is not necessarily in the form of well developed filaments, but forms a contiguous cold water mass of some extent.

42

**FIGURE 4.7** The 14h00 wind-run as recorded at Cape Point (a) and Cape Agulhas (b) for January, 1982. The solid lines represent those days for which suitable satellite imagery was available. There was no upwelling between Cape Point and Cape Agulhas over this period.

43

**FIGURE 4.8** The 14h00 wind-run diagrams at Cape Point (a) and Cape Agulhas (b) during July, 1985. The dotted lines indicate those periods where satellite data are not available. The horizontal lines extending from the black dot indicate the linear distance that the upwelling extended west-, east- and southwards from a reference point (represented by the dot) located at the centre of Walker Bay for the dates shown.

44

**FIGURE 4.9** The 14h00 wind-run diagrams from Cape Point during January 1984. The dotted lines indicate those periods where satellite data are not available. The horizontal lines extending from the black dot indicate the linear distance that the upwelling extended west-, east- and southwards from a reference point (represented by the dot) located at the centre of Walker Bay for the dates shown.

45

**FIGURE 4.10** The 14h00 wind-run diagrams from Cape Point (a) and Cape Agulhas (b) during February 1984. The dotted lines indicate those periods where satellite data are not available. The horizontal lines extending from the black dot indicate the linear distance that the upwelling extended west-, east- and southwards from a reference point (represented by the dot) located at the centre of Walker Bay for the dates shown.

45

**FIGURE 4.11** The daily minimum sea temperatures as recorded in Betty's Bay at a depth of 8 metres for January (above) and February (below), 1984.

46

**LIST OF TABLES.**

	PAGE
<b>TABLE 2.1</b> The monthly averaged distances at which the upwelling front occurred off Lüderitz and Cape Town for the years 1979 and 1982 to 1985.	16
<b>TABLE 3.1</b> : Dates of observed sand plume activity and the associated filament activity at Lüderitz between 1978 and 1984.	23
<b>TABLE 3.2</b> The average daily filament occurrence for each month for the area between Cape Town and 30°S and the coastal strip 5° of latitude either side of Lüderitz.	30
<b>TABLE 3.3</b> Orientation and location of the filament axes off Lüderitz. The distances are measured with Lüderitz being a value of 0. Each axis was extended landwards to the 15°E line of longitude. The "+" indicates the distance the extended axes struck this latitude south of Lüderitz, while the unsigned values indicate the distance to the north. The "-" represents those months when the data were insufficient to identify the axis angle or where no apparent axis could be resolved.	31

**LIST OF TABLES.**

	PAGE
<b>TABLE 2.1</b> The monthly averaged distances at which the upwelling front occurred off Lüderitz and Cape Town for the years 1979 and 1982 to 1985.	16
<b>TABLE 3.1</b> : Dates of observed sand plume activity and the associated filament activity at Lüderitz between 1978 and 1984.	23
<b>TABLE 3.2</b> The average daily filament occurrence for each month for the area between Cape Town and 30°S and the coastal strip 5° of latitude either side of Lüderitz.	30
<b>TABLE 3.3</b> Orientation and location of the filament axes off Lüderitz. The distances are measured with Lüderitz being a value of 0. Each axis was extended landwards to the 15°E line of longitude. The "+" indicates the distance the extended axes struck this latitude south of Lüderitz, while the unsigned values indicate the distance to the north. The "-" represents those months when the data were insufficient to identify the axis angle or where no apparent axis could be resolved.	31

## ABSTRACT

The Benguela upwelling system off southern and south western Africa is a zone of strong and extensive upwelling. Owing to the greater fish numbers found along the front between the upwelling and South East Atlantic Ocean the frontal zone is a key element in the ecology of the upwelling area. This discourse focuses on the perturbations of this front.

The major data source used was the daily Meteosat satellite imagery for the years 1978, 1979 and 1982 to 1985 in the visible and infrared wavebands. These data enable the investigation of cross frontal activity for the entire Benguela Upwelling System at various spatial and temporal scales. NOAA satellite infrared imagery was also used.

At the macroscale two upwelling zones are described. The first is the upwelling core along the coast which exhibits well-developed and persistent upwelling. Offshore of this is an area in where the more transient filament activity predominates. This outer zone is one of constant change and presents highly variable frontal boundary locations. As far as the persistent upwelling is concerned, the northern boundary closely approximates that suggested by Shannon (1985) of 17°S. Cape Agulhas was the effective southern boundary of any regular upwelling. The mean offshore extent of the outer upwelling is 270 kilometres off Lüderitz and 45 kilometres off Cape Town.

An analysis of the seasonal location of the front shows that the greatest upwelling extent at both Lüderitz and Cape Town is observed in winter. Although the winter upwelling extent is the greater of the two seasons, the summer frontal location at Cape Town, in turn, exhibits remarkable stability. The upwelling off Lüderitz, on the other hand, is prone to almost constant frontal location fluctuations.

Most of the variation occurs as a result of the growth and decay of filaments. Filaments were seen along the entire upwelling zone from Cape Agulhas to Cape Frio. On average, the filament sector was 270 kilometres wide off Lüderitz. Between Cape Point and Cape Agulhas the southwards extent of the upwelling rarely exceeded 40 kilometres, while the maximum filament off Cape Point was about 200 kilometres. A filament at Cape Point generally extends about 40 kilometres westwards and the upwelling zone off Walker Bay stretches about 20 kilometres southwards, onto the Agulhas Bank. Along the coast between Cape Agulhas and Cape Point the filaments rapidly react to changes in the wind speed and direction. Mesoscale weather systems are therefore important factors in determining filament activity there. This also true to some extent at Lüderitz. The berg wind can induce rapid filament growth off Lüderitz.

Despite an upwelling positive wind direction it is the wind speed that determines whether upwelling will develop at Cape Town at all. At Lüderitz the wind speeds appear to determine the cross frontal temperature gradient. The greater the wind speed, the steeper the temperature gradient. Cross frontal temperature gradient of between 0.02°C and .006°C per kilometre were calculated for Lüderitz, which compares well with readings in the Californian upwelling zone (Koblinsky et al. 1984).

In the way filaments extend the length of the frontal zone greatly and the manner in which these cold water streams react to the changing winds, they are complex upwelling frontal features of great variability and importance in the Benguela upwelling system.

**CONTENTS**

<b>DECLARATION</b>	i
<b>ACKNOWLEDGEMENTS</b>	ii
<b>LIST OF FIGURES</b>	iii
<b>LIST OF TABLES</b>	vii
<b>ABSTRACT</b>	viii
<b>CHAPTER ONE</b>	<b>1</b>
<b>THE GENERAL UPWELLING ENVIRONMENT OF THE SOUTHERN AFRICAN SUBCONTINENT</b>	
1.1 INTRODUCTION.	1
1.1.1 Study Area.	3
1.1.2 The Upwelling Process.	3
1.2 THE PHYSICAL UPWELLING ENVIRONMENT.	4
1.2.1 Meteorology of the Benguela Upwelling System.	5
1.2.2 Macroscale Bathymetry.	6
1.2.4 Mesoscale Bathymetry.	6
1.2.5 Water Masses.	7
1.3 PROBLEM STATEMENT.	7
1.5 STRUCTURE OF THE THESIS.	9
<b>CHAPTER TWO</b>	<b>10</b>
<b>THE MACROSCALE FRONTAL MORPHOLOGY</b>	
2.1 DELIMITATION OF THE UPWELLING REGIME.	10
2.1.1 The Dichotomous Upwelling Regime.	11
2.2 LATITUDINAL BOUNDARIES OF THE UPWELLING.	15
2.3 ZONAL BOUNDARIES OF THE UPWELLING.	16
2.4 SMALLER UPWELLING FEATURES.	17
2.5 CONCLUSIONS.	18
<b>CHAPTER THREE</b>	<b>19</b>
<b>THE GEOGRAPHY OF WEST COAST UPWELLING FILAMENTS</b>	
3.1 ANATOMY OF UPWELLING FILAMENTS.	19
3.2 CAUSES OF FILAMENTS.	19
3.2.1 Mesoscale Wind Systems.	19
3.2.1.1 Coastal Lows	20
3.2.1.2 Daily Winds	20
3.2.1.3 Berg Winds	22
3.2.1.4 Ten Day Wind-Stress Vectors Analysis	24
3.2.2 Mesoscale Perturbations.	25
3.2.3 Frontal Jets.	27
3.3 THE PROPERTIES OF FILAMENTS.	27
3.3.1 Sea Surface Temperatures.	27
3.3.2 Filament Frequency.	29
3.3.3 Filament Tracks.	31
3.4 CONCLUSIONS.	32

<b>CHAPTER FOUR</b>	<b>34</b>
<b>SOUTHERN CAPE UPWELLING</b>	
4.1 ANATOMY OF A CAPE FILAMENT.	35
4.2 PHYSICAL FACTORS IN CAPE UPWELLING.	35
4.2.1 Bathymetry.	35
4.2.2 Coastal Topography.	36
4.2.3 Influential Wind Systems.	37
4.2.3.1 Macroscale Winds.	37
4.2.3.2 Mesoscale Winds.	37
4.2.3.3 Bud-off Highs.	37
4.2.3.4 Temperate Cyclones.	38
4.3 DETERMINATION OF FILAMENT ACTIVITY.	38
4.4 GENERAL UPWELLING REGIME	39
4.4.1 Meridional and Zonal Extent of Upwelling.	40
4.5 RECURRING UPWELLING PATTERNS.	41
4.5.1 Case Studies.	43
4.5.1.1 Non-Upwelling Conditions.	43
4.5.1.1.1 January, 1982.	43
4.5.1.1.2 July ,1985.	44
4.5.1.2 Extensive Zonal Upwelling.	46
4.5.1.2.1 January and February, 1984.	46
4.6 CONCLUSIONS.	47
<b>CHAPTER FIVE</b>	<b>49</b>
<b>SUMMARY and CONCLUSIONS</b>	
<b>REFERENCES</b>	<b>53</b>
<b>APPENDIX 1: Papers and publications arising from this research.</b>	<b>58</b>
<b>APPENDIX 2: Graphs of the daily filament frequencies at Lüderitz between 1979 and 1985.</b>	<b>59</b>
<b>APPENDIX 3: Graphs of the daily filament frequencies at Cape Town between 1979 and 1985.</b>	<b>65</b>
<b>APPENDIX 4: Weekly sea surface temperature distribution as recorded by the merchant shipping during July, 1982.</b>	<b>71</b>

## CHAPTER ONE

### THE GENERAL UPWELLING ENVIRONMENT OF THE SOUTHERN AFRICAN SUBCONTINENT

#### 1.1 INTRODUCTION.

Upwelling is probably the most significant oceanic phenomenon found on the eastern coastal boundaries of all the major oceans. Of the five major systems (Figure 1.1), that which is found off the coast of southern Africa, the Benguela upwelling system, is investigated here.

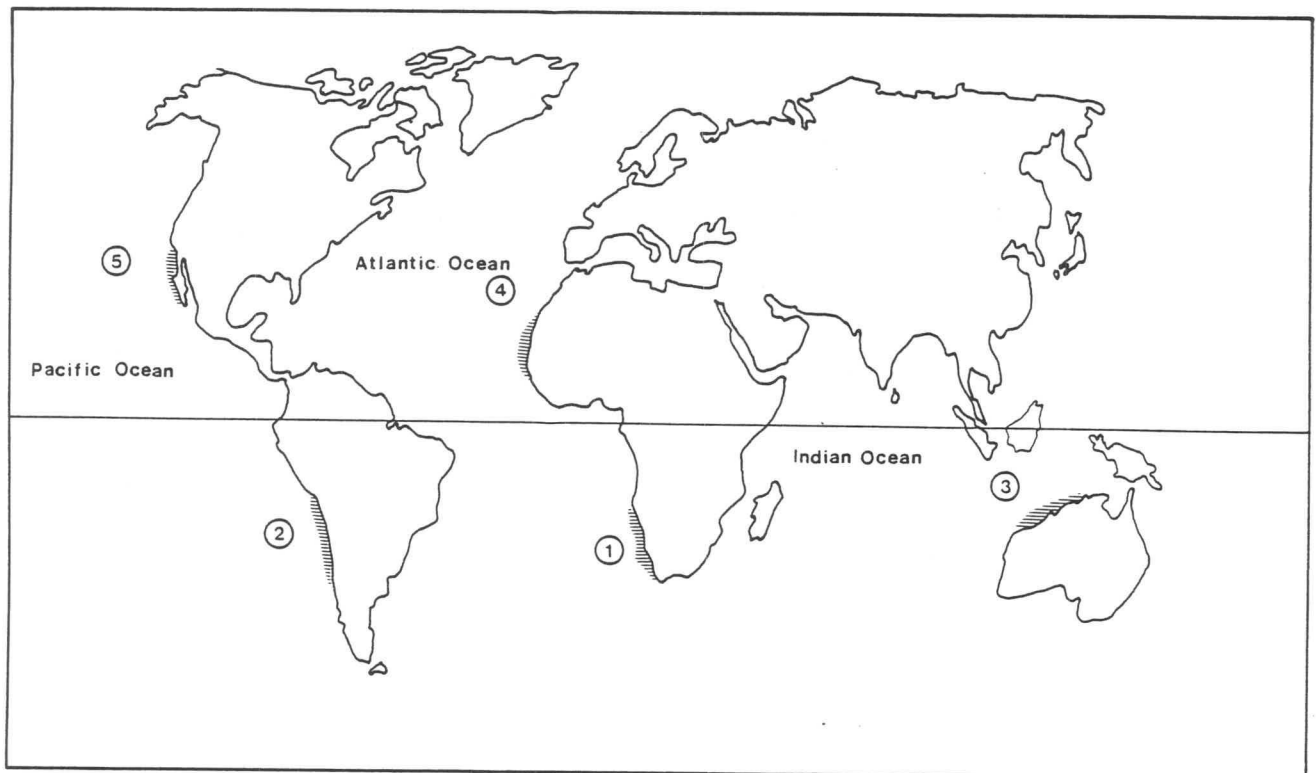


FIGURE 1.1 The locations of the major upwelling zones of the world ;

- (1) Benguela Upwelling system;
- (2) Chile and Peruvian Upwelling area;
- (3) Northwestern Australian Upwelling zone;
- (4) North African Upwelling regime;
- (5) Californian Upwelling system.



### 1.1.1 Study Area.

The Benguela upwelling system off southern and south western Africa, from Cape Agulhas to Cape Frio, (Figure 1.2) which is an ocean area of particularly strong and extensive upwelling.

### 1.1.2 The Upwelling Process.

Upwelling is the process by which cold subsurface water ascends to the surface in response to the removal of the upper water layers by divergent horizontal flow. This flow results when wind blows equatorwards along a coastline with the land to the right (in the southern hemisphere) causing an offshore transport in the oceanic Ekman layer (Figure 1.3 (b) and (c)). The upward motion of the near coastal bottom waters is required to supply this transport and therefore to conserve mass (Perry and Walker 1977 and Brink 1983). This leads to a thermal upwelling front between the cold upwelled water abutting the coast waters and the warmer water of the ocean basin. This front displays strong gradients in horizontal density and temperature at the sea surface (Figure 1.3 (c)).

The rising cold water is rich in inorganic nutrients from the layers below the euphotic zone. These

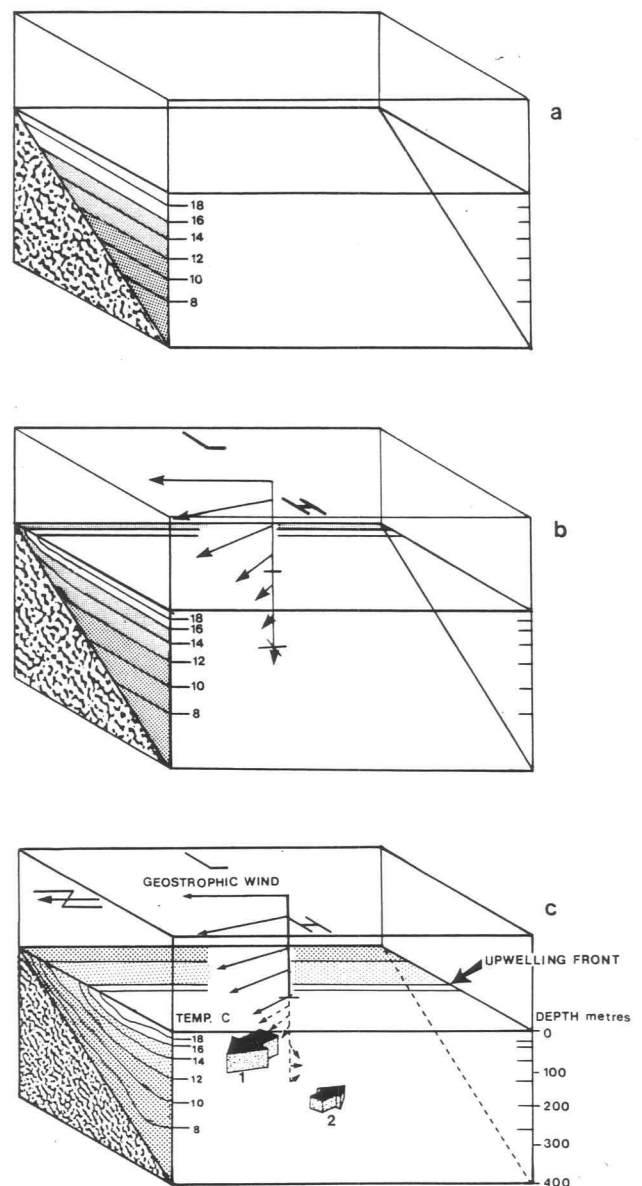


FIGURE 1.3 A schematic diagram of the upwelling process as found off the western margins of most major landmasses in the southern hemisphere. (a) Indicates a theoretical inactive phase where there is no longshore wind. The isotherms are horizontal. (b) With the onset of a longshore wind an Atmospheric Ekman spiral results in the wind stress applied to the water surface being slightly offshore. (c) The spiral continues below the surface resulting in the mean mass transport of the water being offshore (1). This is compensated for by a return flow (2) at deeper levels, forcing the cold water to the surface along the coastline.

nutrients are conducive to phytoplankton growth. The phytoplankton blooms act as fodder for the physiologically more complex zooplankton. The zooplankton are in turn consumed by larger organisms in the classic foodchain, resulting in the valuable pelagic fish stocks associated with the upwelling zone. This productive biomass is not distributed evenly over the geographic area of an upwelling cell but is concentrated in the vicinity of the upwelling front (Simpson et al. 1979, Dengler 1985 and Shannon et al. 1985). This is similar to the findings of enhanced phytoplankton pigment and organism concentrations at continental shelf-edge fronts (Marra et al. 1982, Pingree et al. 1982), at deep-sea fronts (Planke 1977, Allanson et al. 1981, Lutjeharms et al. 1985) and at the borders of other circulation features such as Gulf Stream rings (Gordon et al. 1982, Olson and Backus 1985, Yentsch and Phinney 1985). The upwelling front is therefore probably a key element in the ecology of the area.

## 1.2 THE PHYSICAL UPWELLING ENVIRONMENT.

The Benguela upwelling front is not a regular feature, but is subject to numerous perturbations which result in a dynamic and convoluted thermal divide. The meandering form of this front was first described by Currie (1953) who suggested that this might relate to the existence of specific centres of cold subsurface water. These centres of localised upwelling have been confirmed by numerous studies (Shannon 1985). Their geographical locations have been plotted by Lutjeharms and Meeuwis (1987) (Figure 1.4).

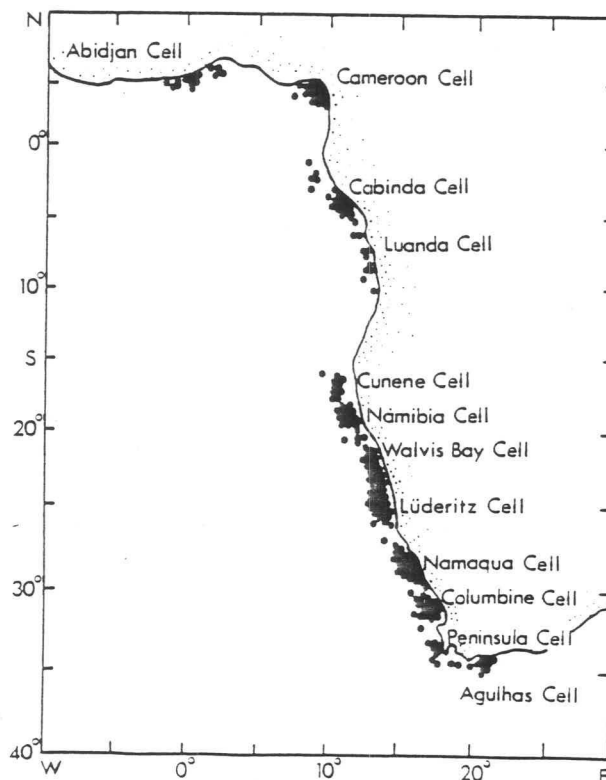


FIGURE 1.4 Geographic distribution of identifiably distinct upwelling cells in the South-East Atlantic Ocean. Each dot represents the centre of an upwelling event observed over a period of 156 weeks. (Lutjeharms and Meeuwis, 1987)

Seasonal and short-term fluctuations in the location and intensity of the upwelling front may govern primary food production and therefore influence the fishing potential of the zone. Over the longer term, warm events occurring on time scales of about 10 years may also temporarily diminish the upwelling-induced food production (Walker et al. 1984).

Notwithstanding the recognised key role the frontal area plays, the nature of perturbations in the frontal zone are not yet fully understood. What is known, however, is that the extent of the zone influenced by the upwelling varies seasonally. These meteorologically induced seasonal variations enable the classification of the numerous upwelling cells (Figure 1.4) into two general regions.

The northern region stretches from the Walvis Ridge, (Figure 1.2) abutting the African coastline at about 20°S, down to the mouth of the Orange River (28°30'S) (Shannon 1985). The southern upwelling regime encompasses the coastal strip between the Orange River, southwards and southeastwards to Cape Agulhas (35°S).

#### **1.2.1 Meteorology of the Benguela Upwelling System.**

North of the Orange River curved anticyclonic atmospheric flow at the surface, associated with the South Atlantic Anticyclone (SAA), is guided by the coastline of the subcontinent. Although the coastal topography of this area consists of sand dunes and a gentle seaward slope over most of its length north of Cape Columbine, its desert-like features cause it to act as a thermal barrier to cross-shore flow. Consequently, the ambient winds along this coast blow along the coastline towards the equator, and are therefore perennially favourable to upwelling (Nelson and Hutchings 1983). This upwelling serves to increase the temperature contrast between the coastal waters and the warm land mass, enhancing the thermal gradient. Controls are imposed upon the effects of these thermal driving forces by the altitude of atmospheric seasonal inversion over the subcontinent. Furthermore in a stable air mass over a cold water body, such as that found under the inversion, the wind velocity is inhibited as the water cooling the air reduces the availability of ambient kinetic energy.

The southern upwelling region has a more complex wind regime which is largely related to the seasonal movement of the SAA. In the summer, between October and March, the



The granitic and sandstone outcrops that typify the coastline between Cape Columbine and Cape Agulhas create a coastline characterised by capes and bays. These cause upwelling that is different in nature, persistence and morphology from that found in the north.

#### **1.2.4 Water Masses.**

Subtropical Surface Water is the predominant surface water type in the South-East Atlantic Gyre. Immediately below this water type is the Atlantic Central Water which becomes exposed to the surface during upwelling (Lutjeharms and Valentine 1987). The Atlantic Central Water originates at the Subtropical Convergence Zone, found at about 40° S at the interface of the Subantarctic and Subtropical Waters, by the mixing of these two water types (Darbyshire 1966).

Further modifications in the water characteristics of the upwelling environment take place at the mesoscale over the Agulhas Bank at the interface of the Atlantic and Indian Ocean current systems. Numerous current systems are relevant here. Approaching from the east, the swiftly flowing, warm Agulhas Current runs down the coast aligned roughly along the continental shelf. In the west is the cooler Atlantic Ocean. The routes over which these systems exchange water are complex. There is evidence that warm water advects westwards along the shelf of the Agulhas Bank area with the cold water entering as a deep poleward flow along the coast and also along the 200 metre isobath (Nelson and Polito 1987). The water over the Agulhas Bank is a mixture of these water types. During spring cold water flows over the shelf from the west, remaining there until autumn and upwelling of Central Water can occur close inshore west of Cape Agulhas (Shannon 1985).

The different water types coincide closely with the two zones of coastal bathymetry discussed above, further suggesting the logical division of the upwelling regime into two distinct study areas.

### **1.3 PROBLEM STATEMENT.**

The northern upwelling zone between the mouth of the Orange River and Cape Frio is the more commercially important zone in terms of the pelagic fishing industry. This

probably is because it is the more extensive and persistent of the two regimes. The second regime, that between Cape Agulhas and Cape Columbine (Figure 1.2), is also important to the fishing industry, however, for it may influence the pelagic fish spawning conditions on the Agulhas Bank (Boyd et al. 1985). Thus both areas deserve attention.

While the northern zone has been examined at seasonal and annual time scales (Shannon 1985), little is known about the day-to-day fluctuations of the frontal zone. On the other hand, using NIMBUS imagery the mesoscale, transient upwelling features and frontal distortions have been well described south of Cape Columbine (Andrews and Hutchings 1980, Schumann et al. 1982, Taunton-Clark 1985, Boyd et al. 1985 and Jury 1985). Few investigations done there have endured long enough to determine inter and intra-annual characteristics of these features accurately.

These shortcomings are addressed by using, for the first time, the full six years of daily Meteosat imagery currently available. With these data the following questions concerning cross frontal activity are addressed:

1. What are the macroscale characteristics of the front over the entire Benguela Upwelling System ?
2. What is the nature of the cross frontal features known as filaments at various spatial and temporal scales along the South West Africa/Namibia coastline ?
3. How does the upwelling around the southwestern Cape coast differ from that off Lüderitz ? If this upwelling zone does differ, what are the major large scale spatial and temporal attributes that best describe it ?

Some of the shortcomings in the spatial resolution of the Meteosat imagery are ameliorated by the use of three years of NOAA satellite infrared imagery. In both cases a graphic technique for frontal delineation from satellite imagery, developed for this study, was used. In the case of Meteosat this technique allows a study of the changes in frontal location at the daily, monthly, seasonal and annual time-scales and from the macro to the mesoscale. Although NOAA imagery allows a much finer spatial resolution it is not as frequent as the METEOSAT products.

#### **1.4 STRUCTURE OF THE THESIS.**

The structure of this thesis reflects the intent to systematically tackle the three questions as outlined above. In Chapter Two attention is focused on the macroscale frontal morphology over the whole Benguela Upwelling system. Chapter Three examines the finer scale cross frontal features known as filaments along the coastal margins of the Namib Desert. This chapter includes a case study of a significant frontal event around the Lüderitz area. Chapter Four looks more closely at the southern upwelling region.

## CHAPTER TWO

### THE MACROSCALE FRONTAL MORPHOLOGY

As the productive biomass in the Benguela upwelling regime is concentrated along the frontal zone, an understanding of this zone is important. This is not straightforward, however, as this region is subject to frontal filaments (Brink 1983), eddies and plumes (Feldman 1986) that significantly increase the length of this ocean/upwelling interface.

Such mesoscale features are clearly evident in the satellite image in Figure 2.1. This uncalibrated portrayal of cold, upwelled water off the west coast of southern Africa shows an extremely convoluted upwelling front with a range of plumes, filaments and wisps of cold water streaming offshore. Extensive seaward penetrations of upwelling plumes are visible at Lüderitz and Hondeklipbaai with filaments extending as far as 750 kilometres or more offshore (Van Foreest et al. 1984, Lutjeharms and Stockton 1987). Plumes streaming off the Cape Peninsula and Cape Columbine upwelling cells are well defined and are described in the literature (Jury 1985, Shannon et al. 1985, Taunton-Clark 1985). Images of this nature corroborate statements made 30 years ago (Currie 1953, Hart and Currie 1960) on the convoluted and intricate nature of this upwelling front. Before starting on the detailed study of the features responsible for disturbing the front, it is important to place them in their macroscale context.

#### 2.1 DELIMITATION OF THE UPWELLING REGIME.

Because satellite imagery allows the regular monitoring of cross frontal features on a space and time scale not feasible before, it has been extensively used for this study. Two sources of satellite imagery were used. The primary source consisted of daily thermal infrared images in the 10,5-12,5 micrometre waveband from METEOSAT I and II for the years 1978 - 1979 and 1982-1985. Data were received directly at the Satellite Remote Sensing Centre of the CSIR at Hartebeesthoek in the Transvaal and suitably contrast-enhanced. The spatial resolution achieved by METEOSAT in the thermal infrared is 5 x 5 kilometres at nadir on the equator but, because of the distance and distortion from the curvature of the earth, considerably poorer in the area of interest. The second source of data was the polar-orbiting NOAA-9 satellite, from which a representative image is given in Figure 2.1. Sampling resolution along the subsatellite track in this instance is about 900 x 900 metres in the 10,5 to 11,5 micrometre infrared waveband. Appropriate contrast enhancement was also carried out for these images. No atmospheric corrections or thermal calibration were made for either data sets so that the resultant portrayals of temperature differences are not absolute.

For the major part of the analysis daily METEOSAT images in the form of photographic negatives were interpreted when and wherever they were sufficiently cloud-free. The line of greatest grey-scale contrast in the South-East Atlantic Ocean was assumed to be the main surface expression of the frontal boundary between the cold upwelled water and the offshore South Atlantic Surface Water. Even though such interpretation is partially subjective, experience has shown (J J Agenbag, Sea Fisheries Research Institute, pers. comm.) that the thermal gradients at these fronts are such that enhancement changes or application of different calibration algorithms in most cases have little effect on the perceived geographic location of boundaries.

Nevertheless, the contrast fluctuation occurring from day to day as a result of changes in the water vapour content of the atmosphere and contrast-enhancement changes were accommodated by reference to the location of the front on the previous three days. The few cases in which excessively rapid shifts were observed which might have been due to the above factors were discarded. All the geometric projections used for this study are those of METEOSAT. The entire west coast upwelling area from Cape Agulhas to 20° S was considered. These boundaries were chosen to include the outer limits of the upwelling suggested by Shannon (1985).

### **2.1.1 The Dichotomous Upwelling Regime.**

From Figure 2.1, the macroscale South-East Atlantic upwelling regime may be seen at any one time to be categorised as consisting of a fully fledged, contiguous coastal upwelling strip, as well as an offshore area consisting of a collection of plumes, streamers, eddies and filaments. This dichotomous division resembles that discussed by Schell (1970). That such a classification is not inconsequential is demonstrated by the geographic extent of each separate regime shown in Figures 2.2 and 2.3 for each season.

Figures 2.2 and 2.3 were constructed by drawing an envelope around the upwelling area along the frontal boundary for each day on which data were available. The inner border of this envelope shows the limit of the seaward extent of the area of unbroken upwelled water during these periods; the outer boundary delimits the farthest seaward extent of any frontal protuberances. This outer boundary therefore included the extensions of all filaments, plumes and other cold mesoscale features for any specific day.

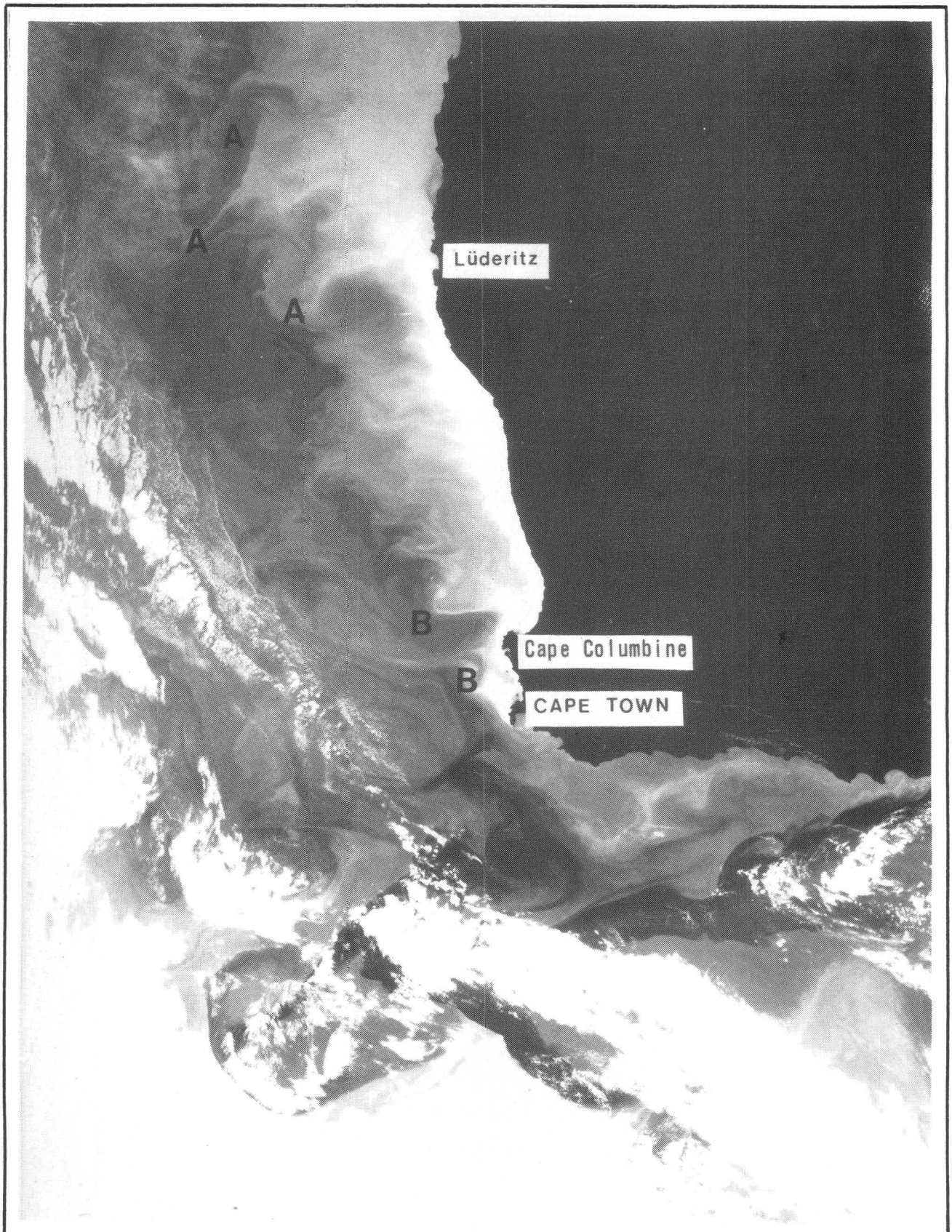


FIGURE 2.1 Thermal infrared satellite image of the South East Atlantic Upwelling system, showing detail of the upwelling front on 26 May 1986. Mesoscale features apparent are the deep sea frontal filaments (A), and the cape filaments (B).

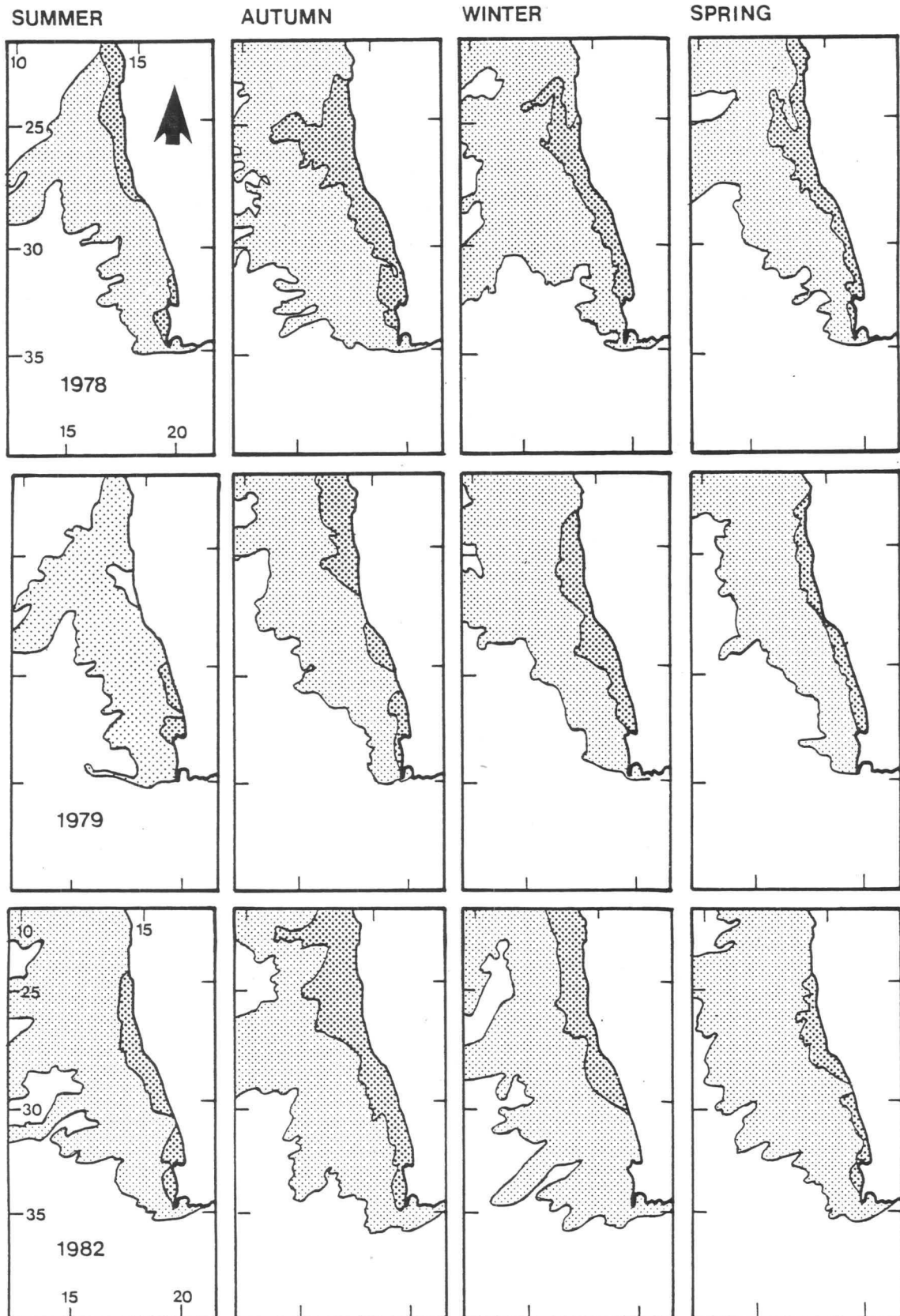


FIGURE 2.2 The seasonal location of the upwelling core along the west coast of southern Africa (dark shading) and the amorphous, active frontal zone (lighter shade) for 1978, 1979 and 1982. The Meteosat satellite for this area was not operational during 1980 and 1981.

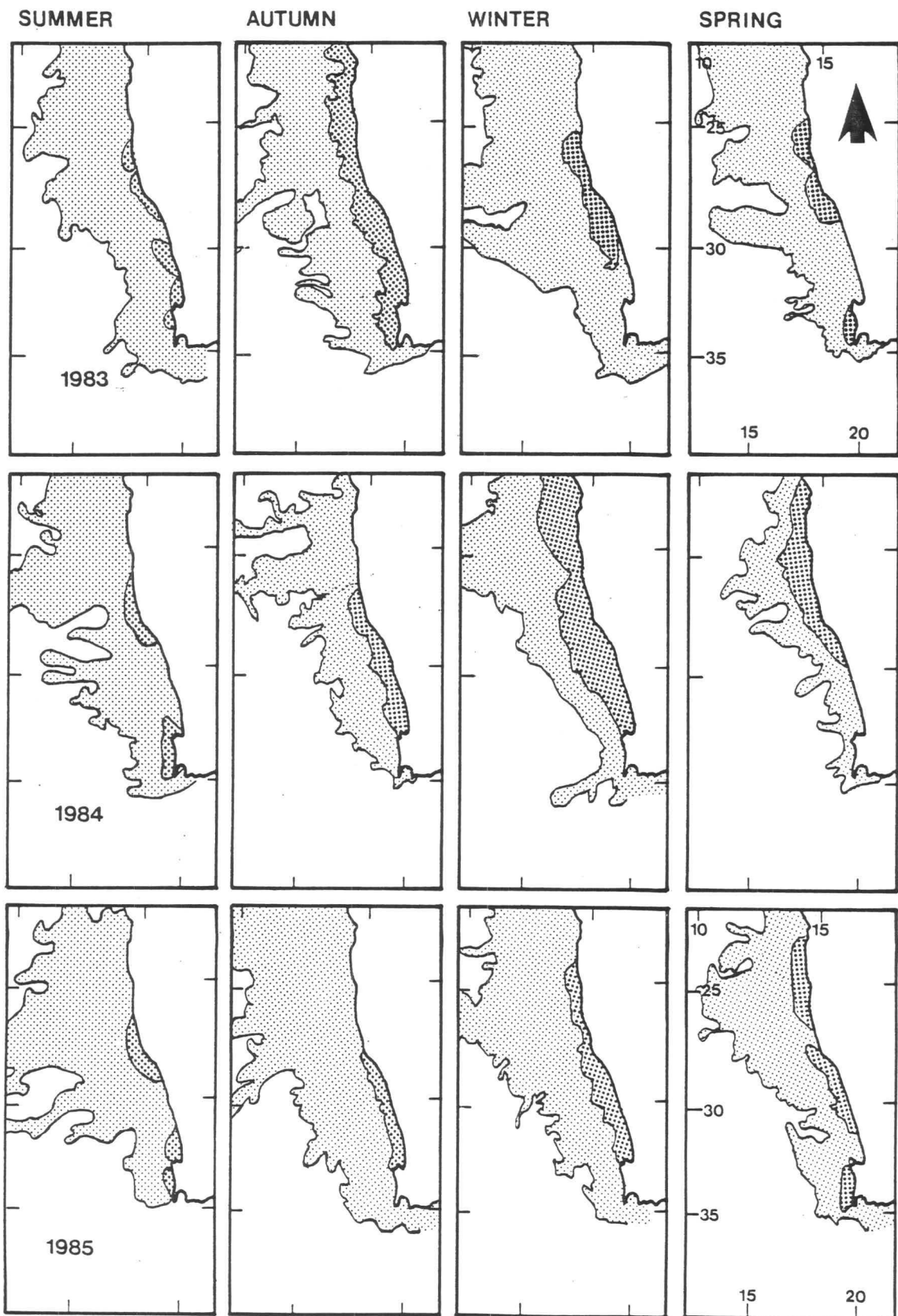


FIGURE 2.3 The seasonal location of the upwelling core along the west coast of southern Africa (dark shading) and the amorphous, active frontal zone (lighter shade) for 1983, 1984 and 1985.

The daily frontal positions were overlaid for each calendar month. These monthly overlays were then grouped into four seasons;

- i) Summer - December (of the previous year), January and February
- ii) Autumn - March, April, May.
- iii) Winter - June, July, August.
- iv) Spring - September, October, November.

The results clearly show the seasonal latitudinal and zonal patterns of the upwelling.

## 2.2 LATITUDINAL BOUNDARIES OF THE UPWELLING.

Shannon et al. (1987) have described the northern borders of the upwelling regime, the Angola-Benguela front, in some detail from historical hydrographic as well as remotely sensed data. They conclude that the location of this front may vary seasonally between 15° and 17° S. Parrish et al. (1983) also place the average northern boundary at 15° S. With belts of wind stress conducive to upwelling shifting seasonally and interannually, an invariant boundary is not to be expected.

In his summary of previous work in this regard, Shannon (1985) comes to the conclusion that 15°S latitude is the effective northernmost boundary, although previous workers (Copenhagen 1953, Nelson and Hutchings 1983) placed it even farther south. Even the 17°S boundary later suggested by Shannon et al. (1987) may be too far south. The more persistent near-coastal core upwelling extends equatorwards beyond 20°S in seven of the eighteen seasons. The five most extensive upwelling events seen north of this suggested latitude occurred during winter and autumn. Therefore, considering that upwelling occurs regularly north of 20°S latitude, the conclusion reached by Moroshkin et al. (1970) that the actual northern-most boundary of the upwelling may be north of 15°S has some merit.

However, as the surface area delimited by the transient outer upwelling is much greater and often extended outside the boundaries set on the study area, the actual boundary could not be accurately ascertained.

The southern extreme to the Benguela upwelling regime is usually considered to be at Cape Point. Mounting evidence of the active upwelling regime east of Cape Point suggests that this convention may no longer be valid. Schumann et al. (1982) have documented upwelling east of Cape Agulhas and Lutjeharms and Meeuwis (1987) have noted a well-defined upwelling cell off this Cape (Figure 1.4). Figures 2.2 and 2.3, furthermore show, that the upwelling failed to occur at Cape Agulhas only in the spring

of 1978 and the summer of 1985. It would therefore not be unreasonable to consider Cape Agulhas as having a claim to the title of the southern boundary of the Benguela upwelling system. The location of the zonal boundaries of the upwelling are similarly not as clearcut.

### 2.3 ZONAL BOUNDARIES OF THE UPWELLING.

From the qualitative depiction of the upwelling zones two major upwelling regimes were identified for closer inspection. The first area is that off Lüderitz. Being the most extensive in space and time and most active, this upwelling cell was considered to be the primary west coast upwelling subsystem (Lutjeharms and Meeuwis 1987). A plume or stream of some magnitude usually occurs across this front (Lutjeharms and Stockton 1987). For comparison a secondary system at the Cape Peninsula was investigated.

In both cases measurements of the linear distance between the coastline and the front were taken parallel to the lines of latitude, stemming from Lüderitz and Cape Town. These data, averaged for each month are presented in Table 2.1.

Table 2.1 The monthly averaged distances at which the upwelling front occurred off Lüderitz and Cape Town for the years 1979 and 1982 to 1985.				
Month	Lüderitz		Cape Town	
	Distance from Shoreline (km)		Distance from Shoreline (km)	
	Mean	Mode	Mean	Mode
January	234	200	40	30
February	205	250	49	30/45
March	273	200/350	59	60
April	317	250	45	45
May	298	275	42	75
June	320	325	33	45
July	292	275	70	45
August	295	225	53	45
September	286	250	47	30/60
October	196	225	23	30
November	243	200	34	30
December	263	275	44	35
Mean	269		45	

The upwelling off Lüderitz follows the seasonal pattern suggested by Shannon (1985). There is a distinct enlargement in the surface area of the upwelling in autumn in the northern upwelling region with the most extensive upwelling mean seen between April and June (Table 2.1). If one considers the modal filament extents, the winter peak is even more pronounced (Table 2.1). This also true of the southern upwelling region. The

upwelling in the south shows remarkable constancy in summer with a modal extent varying only between 30 and 35 kilometres from October to January (Table 2.1). As the upwelling occurs in response to favourable wind forcing (Andrews and Hutchings 1980, Nelson 1985, Taunton-Clark 1985), this would indicate the small variation within the windfield experienced here during summer. In winter the passage of the low pressure cyclonic systems cause a much more variable wind regime. Therefore a greater zonal range to the upwelling front in that area is to be expected (Brink 1987). The greater intraseasonal variation seen in the distances of the front from Lüderitz is as a result of this area not being as exposed to the distinctly seasonal weather systems that occur at Cape Town. At Lüderitz the dominance of the South Atlantic Anticyclone (SAA) as the major upwelling force is not regularly eroded by a seasonal array of midlatitude depressions. On the contrary, upwelling induced by the winds blowing around this high pressure system may be reinforced during winter by the effects of shallow cyclonic eddies in the atmosphere that move along the coastline of southern Africa. A further contributory factor to the persistence of the upwelling at Lüderitz may be the general location of the front about 270 kilometres out to sea.

Kamstra (1985) has demonstrated that the winds are at their strongest approximately 200 to 300 kilometres offshore. This wind field overlies the mean distance that the outer upwelling envelope is found off Lüderitz (Table 2.1). Parrish et al. (1983), also show that the maximum wind stress over the upwelling system lies in a band offshore. Such a wind-stress configuration would be particularly conducive to forming streamers and perturbations on the main upwelling front as shown in Figure 2.1 (Lutjeharms and Stockton 1987). It would not be as effective in those areas of limited upwelling, found particularly in the south.

#### **2.4 SMALLER UPWELLING FEATURES.**

Note may also be taken of the fact that filaments and plumes seem to exhibit a tendency to extend farthest offshore at Cape Frio, the Lüderitz/Walvis Bay and the Namaqua cells (Figure 1.4) (Shannon 1985, Lutjeharms and Meeuwis 1987). Shannon (1985) conjectured that those upwelling plumes that emanate from the Lüderitz and Hondeklipbaai (Namaqua) cells together establish a major environmental barrier, effectively dividing the upwelling system in two.

The cold water distributions displayed in Figures 2.2 and 2.3 suggest that this may be the case in the persistent upwelling region in summer. The outer upwelling zone is a continuous belt of activity, although the preferential zones are readily apparent. These preferential upwelling zones consist of a central primary plume off Lüderitz flanked by

two secondary plumes at Cape Frio and Hondeklipbaai; locations which are in substantial agreement with the key upwelling cells recognized by Shannon (1985) and Lutjeharms and Meeuwis (1987).

## 2.5 CONCLUSIONS.

Cross frontal extrusions into the ocean basins and intrusions into the upwelling regime seem to occur at all the temporal and spatial scales. Although this situation makes the upwelling front an extremely complex feature some general patterns can be identified.

The upwelling can be seen as two entities. Firstly a core zone along the coast which exhibits well-developed and persistent upwelling. Offshore of this is the second area in which filament and related more transient upwelling elements are found. As far as areal extent is concerned, this latter zone is the greater of the two. Just how extensive the outer zone actually becomes could not be precisely determined.

In broad terms, however, the northern boundary of the outer upwelling envelope can be considered as being located somewhere between 15°S and 20°S. That suggested by Shannon (1985) of 17°S is therefore offers an acceptable compromise as to the siting of the actual boundary location. The southern boundary of any permanent upwelling is at Cape Point but the upwelling is regularly seen stretching eastwards to Cape Agulhas. Zonally the upwelling is extremely variable with a range of the average monthly frontal distance of 121 kilometres at Lüderitz and 47 kilometres for Cape Town. The mean extents of 270 kilometres and 45 kilometres for these sites give a good indication of where the front is normally observed.

The trends in seasonal changes in the distance offshore of the front are similar for both Lüderitz and Cape Town. At both these locations there is an increase in the upwelling extent during winter. There is an indication of a short-term increased extent in February and December at Lüderitz, but this still does not equal that measured in winter. The summer frontal location at Cape Town is very stable on the other hand.

While the seasonal patterns shown in Table 2.1, are clear, most of the variation occurs as a result of the growth and decay of the cross frontal streamers, or filaments. Although these features generally have a limited lifespan, they constitute the major areal section of the upwelling regime which makes the study of these mesoscale features important.

## CHAPTER THREE

### THE GEOGRAPHY OF WEST COAST UPWELLING FILAMENTS

There are two distinct types of filaments in the Benguela system. The majority are those found offshore, extending into the deep sea of the South-East Atlantic Ocean, off the coast between Hondeklipbaai and Walvis Bay. It is these that are examined here with specific reference to an extraordinary filament streaming off Lüderitz during 1982. Although comparisons are made between the "deep sea" filaments and those found around the capes in this Chapter, this latter feature is more fully described in Chapter 4.

#### 3.1 ANATOMY OF UPWELLING FILAMENTS.

Filaments are narrow seaward baroclinic jets emanating from the coastal upwelling region which can advect cold water several hundreds of kilometres offshore (Brink 1983, Flament et al. 1985, Lutjeharms and Stockton 1987). They are typically 20 to 50 kilometres wide and are often accompanied by a seaward jet of between 50 and 80 cm/s (Kosro and Huyer 1985). The surface presentation of the filament is normally asymmetric (Flament 1988). In the Californian upwelling system the steeper front is found on the equatorward side of the filament. This is contrary to the situation shown in Figure 2.1 and numerous other images examined that show filaments in the Benguela upwelling system, such as that seen in 1982 (Figure 3.4).

#### 3.2 CAUSES OF FILAMENTS.

While Ekman divergence may be used to explain the upwelling in general terms (Figure 1.3), there are many other factors which appear to be implicated in the formation of filaments and eddies.

##### 3.2.1 Mesoscale Wind Systems.

During constant favourable alongshore winds a uniform front is created and maintained as seen in the upwelling off Cape Town during summer (Table 2.1). During a lull in these favourable winds the front tends to become more irregular (Brink 1983). This may

result from perturbations associated with strong land and sea breezes, passing coastal low pressure cells and other variable wind systems, the effects of which were also seen in the upwelling zone north of Cape Columbine by Hart and Currie (1960).

#### 3.2.1.1 Coastal Lows.

Of the mesoscale wind systems the coastal low, often preceded by strong offshore east winds which are followed by onshore westerlies, probably contributes greatest to frontal disruption. Coastal lows, as do the land and sea breezes, cause rapidly changing wind shear on the sea surface over a period of hours. The effect of this on upwelling filament dynamics may be seen by examining the reaction of the 1982 filament to the daily fluctuations in the winds blowing at Lüderitz (Figure 3.1).

#### 3.2.1.2 Daily Winds.

The wind speed and direction measured at Lüderitz on each day at 14h00 during 1982 was plotted (Figure 3.1). For ease of reference the length of the filament for any given day on which this could be measured was plotted alongside the wind run diagrams. This Figure shows the influence of daily winds in the determination of the upwelling extent.

During January 1982 the filament reached a length of 800 kilometres. The wind blew steadily from  $160^\circ$  from the first of January, 1982 to the ninth. The wind veering from  $160^\circ$  to  $220^\circ$  between the ninth and eleventh is reflected in the shrinking of the surface expression of the plume by 250 kilometres on the twelfth (Figure 3.1). The renewed onset the wind from  $160^\circ$  on the eleventh is reflected in the restoration of the 250 kilometre filament extent previously lost. A pattern of a one to two day lag between changes in wind direction and a visible reaction in filament length became apparent. As the wind measurements and Meteosat imagery were recorded within a few hours of each other, a change in wind direction on one day would only show on the imagery of the next. Consequently the response of the filament to changes in the wind is often less than 24 hours.

The filament showed an apparent accelerated advection during easterly wind between 31 January and the first of February. Despite the greater persistence in the southeasterly winds, in comparison to that of January, the filament retracted to a length approximately

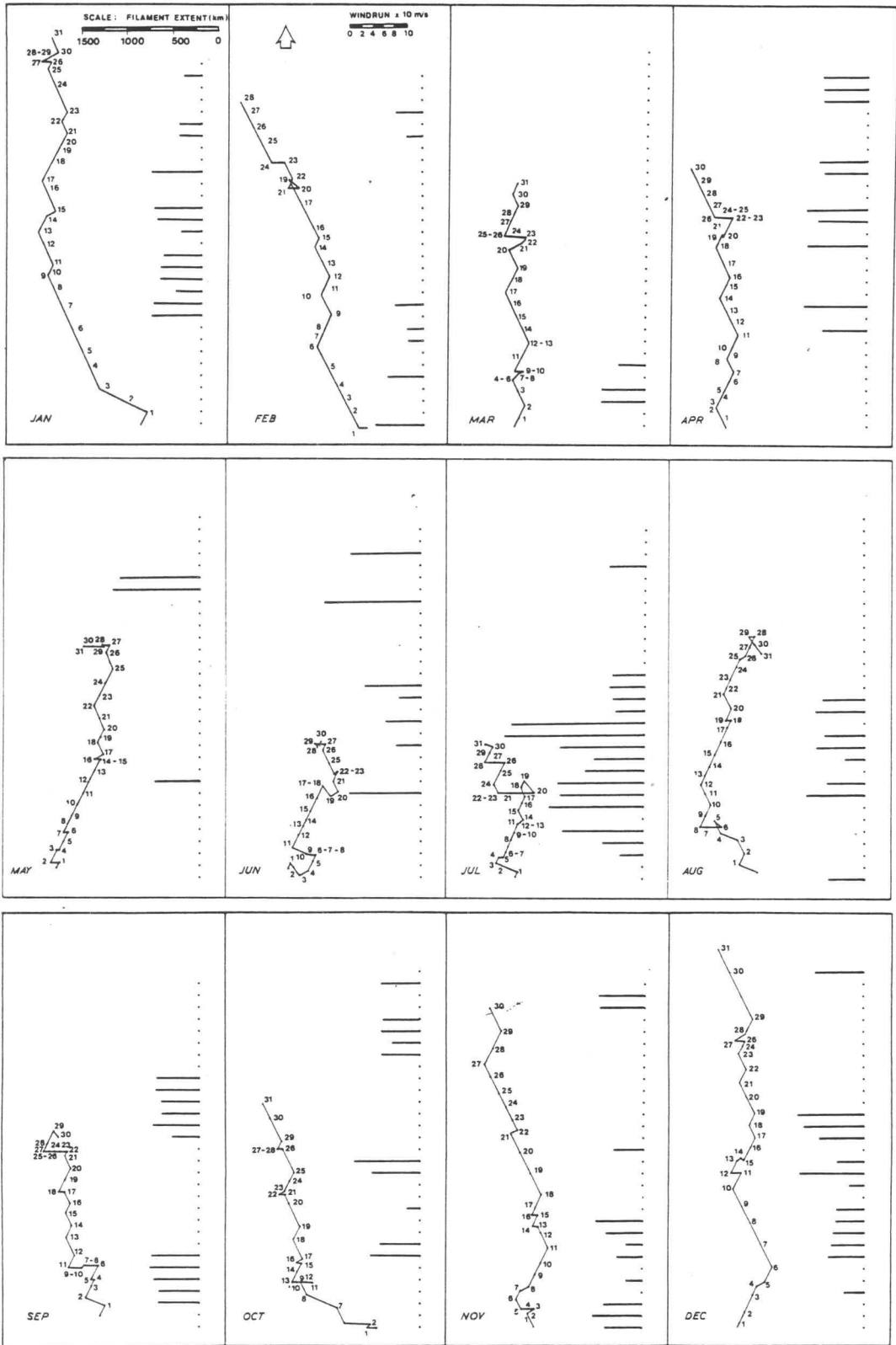


FIGURE 3.1 : Daily wind run diagrams for the 14h00 wind as recorded at Lüderitz during 1982. The stick diagrams show filament extent for each day on which it could be measured. Each day is represented by a dot or stick, starting with the first day of the month at the bottom, progressing to the last day at the top. A dot shows the lack of data for any given day.

300 kilometres shorter at the end of the month than was measured at the beginning. This situation gave little indication of the filament growth that was to follow in the latter parts of March.

The March wind regime was highly variable with regular wind direction changes from the easterly oriented upwelling-favourable winds to the unfavourable westerlies interspersed on two occasions with calm conditions. From this month onwards the general filament extent increased until peaking in July.

Maximum filament extent which was reached after rapid berg wind induced growth between 10 and 12 July (Table 3.1). Overall the winds during July were not as strong as previous months but 10 berg wind, or east wind, days were experienced. The effects of these may be seen on the changing pattern of the sea surface isotherms (Figure 3.5).

The filament decayed by 1150 kilometres on 14 July. The influence of the east wind blowing between 20 and 23 July, ending in a period of calm, can only be surmised, although it may have been partly responsible for the filament pattern of the following week. East winds blew for three of the last seven days of July 1982. The resulting isotherm patterns show a well-developed filament with a steep poleward front extending out of the study area (Figure 3.5). Dust plumes resulting from the east winds may have been what prevented the observation of the sea surface from the satellite imagery. Berg winds would therefore appear to be significant in increasing the offshore reach of filaments, or perhaps even in their creation.

#### 3.2.1.3 Berg Winds.

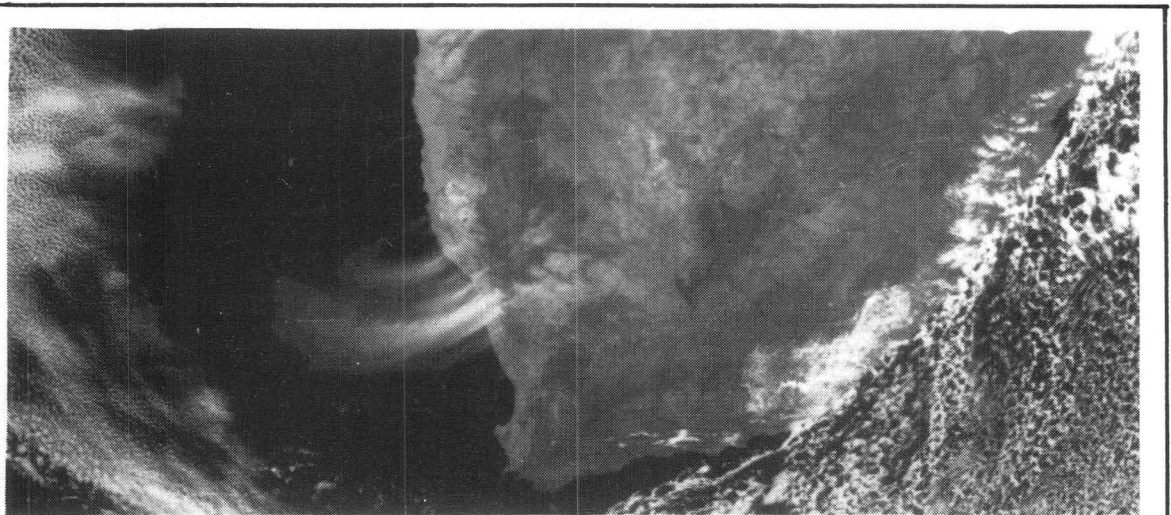


FIGURE 3.2 : Visual waveband image of the west coast of southern Africa of 5 July 1982. The extensive dust-plume resulting from a 30 knot berg wind can be clearly seen being transported out to sea.

Berg winds, blowing from the east, are warm winds associated with an anticyclone over the southern or southeastern part of the continent and a cyclonic depression approaching from the west (Jackson 1951). The anticyclonic circulation around the high results in easterly winds that can exceed 15 m/s (Shannon 1985). On occasion satellite imagery has shown such winds to carry dust and sand about 150 kilometres offshore (Shannon and Anderson 1982) (Figure 3.2). Such events probably represent instances of extremely intense berg winds. A total of twenty-eight images showing dust plumes were extracted from NOAA imagery for the period 1978 to 1984 and tabulated in Table 3.1. On those dates the filament extent off Lüderitz was measured along the filament axis. The same was done for the day preceding and for the two days following the dust storm. These data were then subtracted from the filament extent on the storm day.

TABLE 3.1 : Dates of observed sand plume activity and the associated filament activity at Lüderitz between 1978 and 1984.

Sand plume date	Filament Deviation from extent on;			
	(Day -1)	Event	(Day +1)	(Day +2)
78-06-08	- 75	950	- 500	-
78-06-09	+ 500	450	-	+ 175
78-06-21	0	500	+ 50	+ 150
78-07-06	+ 75	250	-	+ 500
79-05-07	- 75	500	+ 75	+ 250
79-05-08	0	575	+ 175	0
79-05-09	- 175	750	- 175	-
79-05-15	+ 20	450	+ 25	+ 175
79-06-12	-	400	+ 175	+ 175
79-06-13	- 175	575	0	- 25
79-06-14	0	575	- 25	+ 25
79-06-16	+ 50	550	+ 50	+ 50
79-06-17	- 50	600	0	0
79-07-03	+ 100	450	+ 175	- 325
79-10-04	- 125	375	- 25	- 200
82-07-04	- 450	925	+ 475	+ 100
82-07-05	- 475	1400	- 375	- 475
82-07-06	+ 375	1025	- 100	- 350
82-07-11	- 375	925	+ 600	+ 550
82-07-12	- 600	1525	- 50	-1150
83-07-28	- 25	525	+ 325	+ 25
83-08-11	- 85	550	- 150	- 75
83-08-12	+ 150	400	+ 75	+ 200
83-08-23	- 125	625	+ 75	-
84-05-31	0	550	0	-
84-06-22	-	250	+ 200	+ 300
84-06-23	- 200	450	+ 50	- 100
84-07-24	- 50	500	- 150	- 125
Total	-1790	17600	+ 975	- 150
Mean	- 68.8	628.6	+ 37.5	- 6.3

During the berg wind event on 4 and 5 July over the 1982 filament, the water stream advanced in excess of 450 kilometres in 24 hours. While Boyd (quoted in Shannon, 1985) and Jury (pers comm.) consider the berg wind incapable of influencing the upwelling to any significant extent, it is clear that this and those other events able to carry material out to sea are important. From the deviations calculated on 50% of the days when dust plumes occurred as a result of berg winds, there was a growth in the filament extent between the day prior to the onset of the east wind and that measured for the date of the event. In the remaining fourteen cases, seven showed no change in the distance between the shore and the front, while the remaining examples showed a shrinking of the upwelling extent. Where there was an increase, it continues for the day after the sand plume observation. Two days after the event, however, there is a tendency for the cold water stream to contract. Considering the onshore winds associated with the northern sector of coastal low pressure system, this is not unexpected. This shrinkage tends to be less than the magnitude of the growth, resulting in a filament longer than seen before the event. It is clear that the short-term wind fluctuations and short-lived wind systems do influence the finer upwelling structures. This makes accurate results from the application of general rules concerning the relationships between winds and frontal movement unlikely. Nonetheless, the relationship between frontal location and the winds of the previous 10 days, as suggested by Lutjeharms (1981a), was investigated.

#### 3.2.1.4 Ten Day Wind-Stress Vectors Analysis.

Daily wind-run vectors were calculated for a position  $25^{\circ}$  S by  $10^{\circ}$  E in the Atlantic Ocean. This point is considered as the median position of the plume extent for the whole of 1982 and 1984 (Figure 3.3). The wind stress was taken as the square of the geostrophic sea level wind velocity. These data were extracted and extrapolated from the Weather Bureau daily synoptic charts for 1982.

The distance that the main front was found offshore at Lüderitz measured along a line that ran parallel to the line of latitude was used as the dependent variable. Resultants from calculating 10-day running vectors for the wind direction and stress were used as the independent variables. The wind directions were divided into the sixteen standard wind direction classes. Each class was given a value between 4 and -4 rated according to the expected upwelling potential of the wind direction. East winds were given a value of 4 and west winds -4. A multiple regression test carried out on these variables for the year of 1982 showed that changes in the 10-day vectors explained 6% of the variance in upwelling extent. Allowing for errors arising from the generalisations inherent in wind data extracted from synoptic charts, this result is still very poor. The same wind data



were used to investigate the variance in maximum plume length, as measured along the plume axis. An  $r^2$  of 0.21 resulted. These results would suggest that the longer-term winds do not play a significant part in the determination of filament morphology nor in the offshore location of the front. This might explain why despite very similar 10-day wind regimes the filament extent seen in 1984 differed so markedly from 1982 (Figure 3.3). Furthermore, apart from confirming the apparent dominance of the mesoscale weather systems in determining both frontal location and filament dynamics this result raises a key question. What, in fact, sustains the extensive filament as it advects hundreds of kilometres into the ocean basin ?

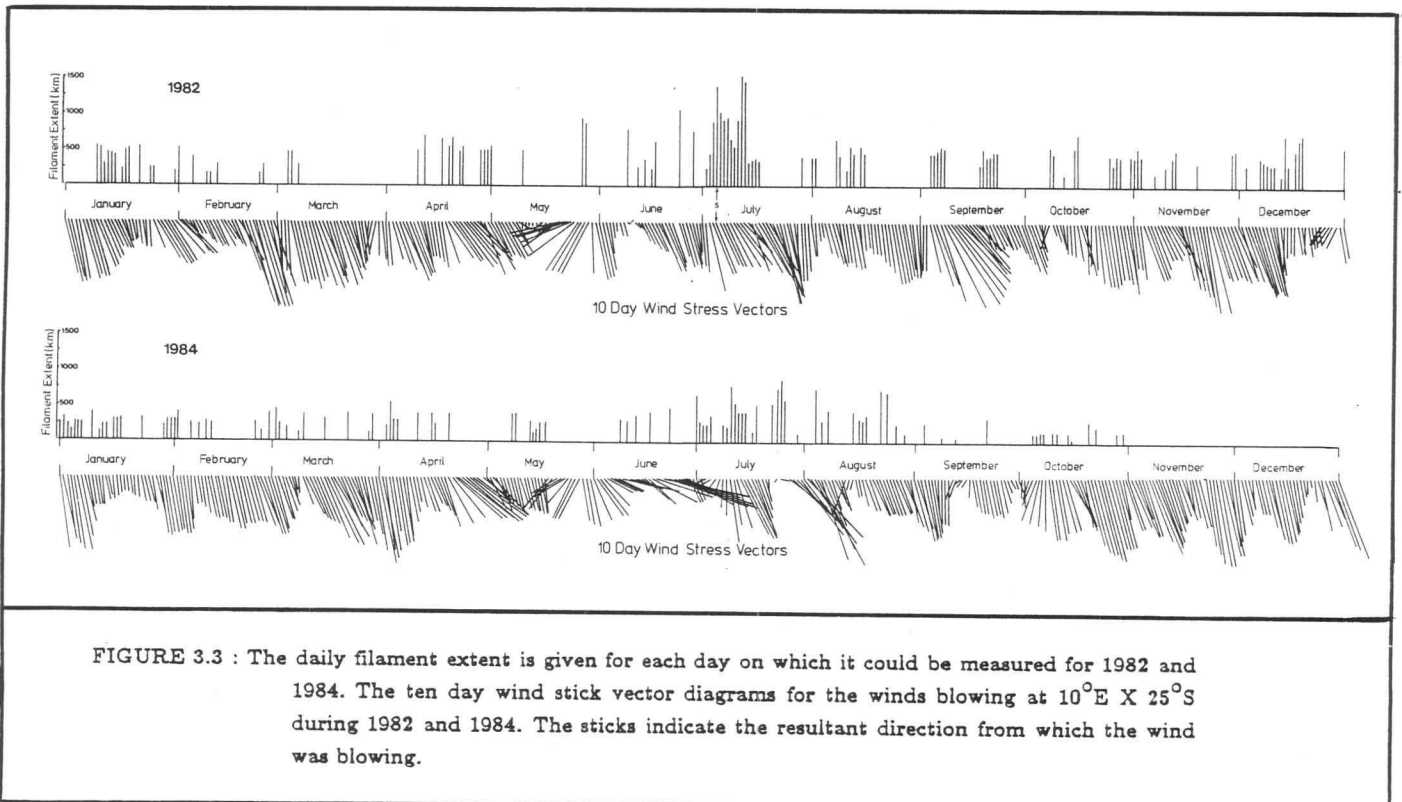
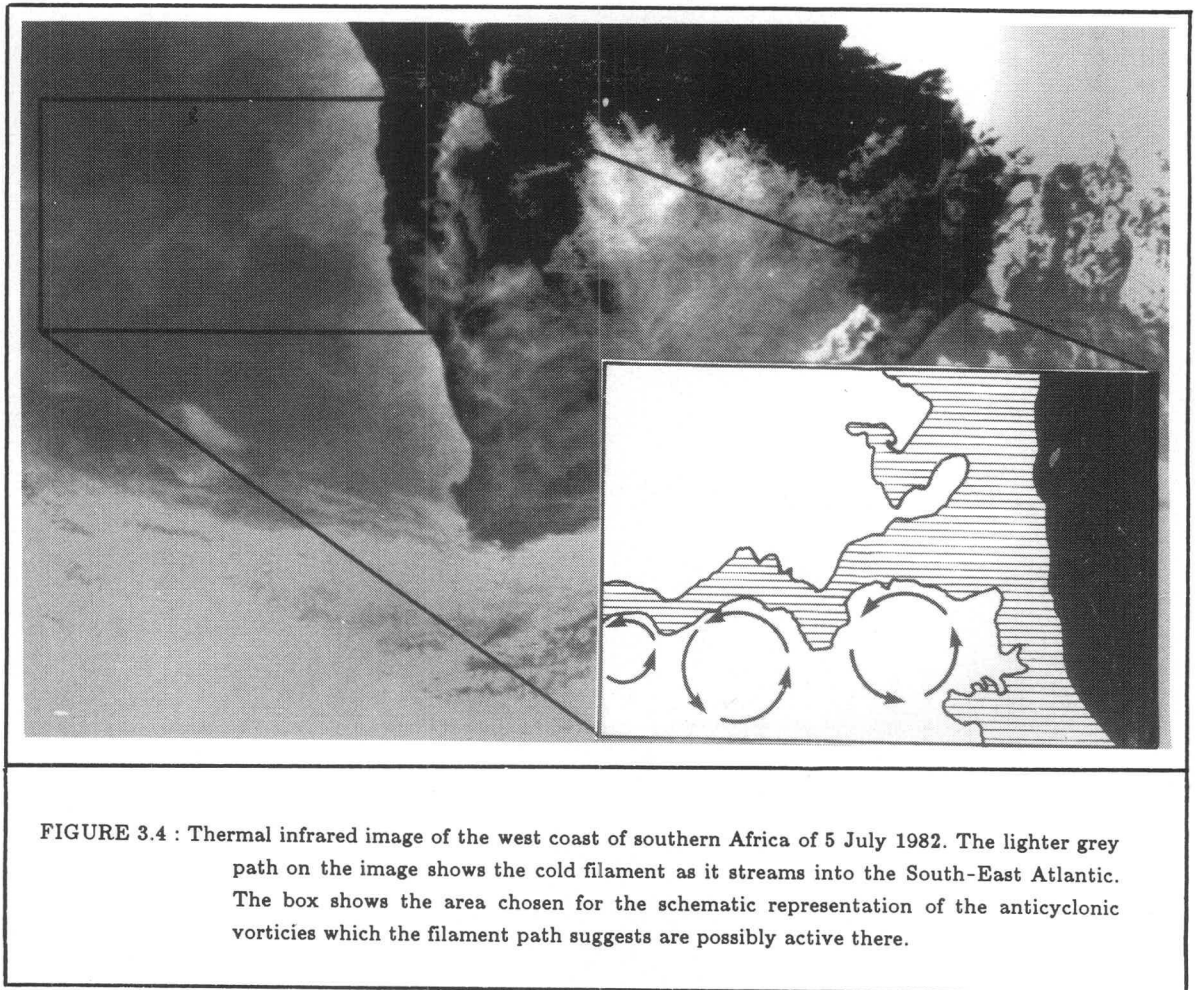


FIGURE 3.3 : The daily filament extent is given for each day on which it could be measured for 1982 and 1984. The ten day wind stick vector diagrams for the winds blowing at  $10^{\circ}\text{E} \times 25^{\circ}\text{S}$  during 1982 and 1984. The sticks indicate the resultant direction from which the wind was blowing.

One solution may lie in mesoscale currents or eddies of the type seen by Mooers and Robinson (1984) within the general Californian Current upwelling system, as well as those seen by Olson and Evans (1986) originating in the Agulhas Current.

### 3.2.2 Mesoscale Perturbations.

After examining Figure 3.4 it does not require too much imagination to accept that the anticyclonic eddies, schematically proposed, could be responsible for the filament morphology seen there. The three arches formed by this filament (Figure 3.4) cannot easily be explained in terms of the prevailing wind. On the other hand, mesoscale eddies



of Agulhas Current origin may well have been present. Lutjeharms (1981b) describes the Agulhas spin-off eddies that are shed as the Agulhas retroflects. These eddies may be similar to the cold-core anticyclonic eddies seen in the Californian Current (Bernstein 1977, Koblinsky et al. 1984). The anticyclonic vorticity associated these eddies of the Northern Pacific was measured to depths of about 1450 metres. It is not inconceivable that an eddy of that nature shed by the Agulhas Current could move up the west coast as far as Lüderitz where their influence may be felt by the more extensive of the filaments. Another, similar, suggestion considers that inherent within the filaments seen along the upwelling front is the tendency to terminate in eddies (Lutjeharms and Stockton 1987, Stockton and Lutjeharms 1988). These are generally cyclonic eddies, but occasional anticyclonic vorticity is seen (Stockton and Lutjeharms 1988). As is the case with the Agulhas rings, such eddies may well be shed into the ocean basin in the process of cross-frontal heat exchange, where they could also act upon the more substantial filaments. All this is largely speculative, however. It is as likely that filament growth is

enhanced by the frontal jets embedded within offshore stream that were reported by Flament et al. (1985).

### 3.2.3 Frontal Jets.

Hart and Currie (1960) found a shelf-edge poleward current at a depth of 200 - 300 metres. Such a flow was seen by Nelson and Polito (1987) around the Cape Peninsula as well. An equatorward current jet at a depth of about 200 metres underlying the upwelling front was identified by Bang (1971). The shear between these diametrically opposed streams could enhance frontal instability. Another explanation may be found in the vorticity imbalance associated with the advection of fluid from high to low latitudes with the dispersion of energy into Rossby waves (Nelson and Hutchings 1983).

## 3.3. THE PROPERTIES OF FILAMENTS.

### 3.3.1 Sea Surface Temperatures.

Sea surface temperature, wind direction and wind velocity measurements for the study area were taken from the SADC database of the CSIR. These data were gathered from the routine weather measurements taken by merchant shipping moving in the normal shipping lanes. As these data leave many key sectors of the area unrecorded and are sparsely distributed, daily plots of the sea surface temperature and winds could not be done. Therefore the data were plotted for each week in July 1982. This period covers the time that the filament appeared to reach its maximum length (Figure 3.5).

From these diagrams the core upwelling is centred around Lüderitz, with temperatures of  $10^{\circ}\text{C}$  appearing to be the norm for this period. The maximum temperature gradient across the front occurred at various distances offshore of this isotherm. During the first week of July the gradient on the poleward side of the filament was  $4^{\circ}\text{C}$  ( $15^{\circ}\text{C}$  to  $19^{\circ}\text{C}$ ) over a distance of about 100 kilometres. Flament et al. (1985) report a very similar temperature gradient on the poleward side of a filament studied off the coast of California. On the equatorward side of that specific filament, the temperature gradient was  $2.9^{\circ}\text{C}$  per kilometre, however.

The general trend over the rest of the upwelling front shows a gradient of  $2^{\circ}\text{C}$  ( $17^{\circ}\text{C}$  to  $19^{\circ}\text{C}$ ) over distances that vary between 100 and 300 kilometres. This is very similar to the mean sea surface temperature gradient measured off California by Koblinsky et al. (1984). The average wind velocity of 9 m/s during this first week of July was the greatest for the month. Between 8 and 15 July the mean wind velocity was 6 m/s. This reflected by evenly spaced sea surface isotherms with no strong frontal

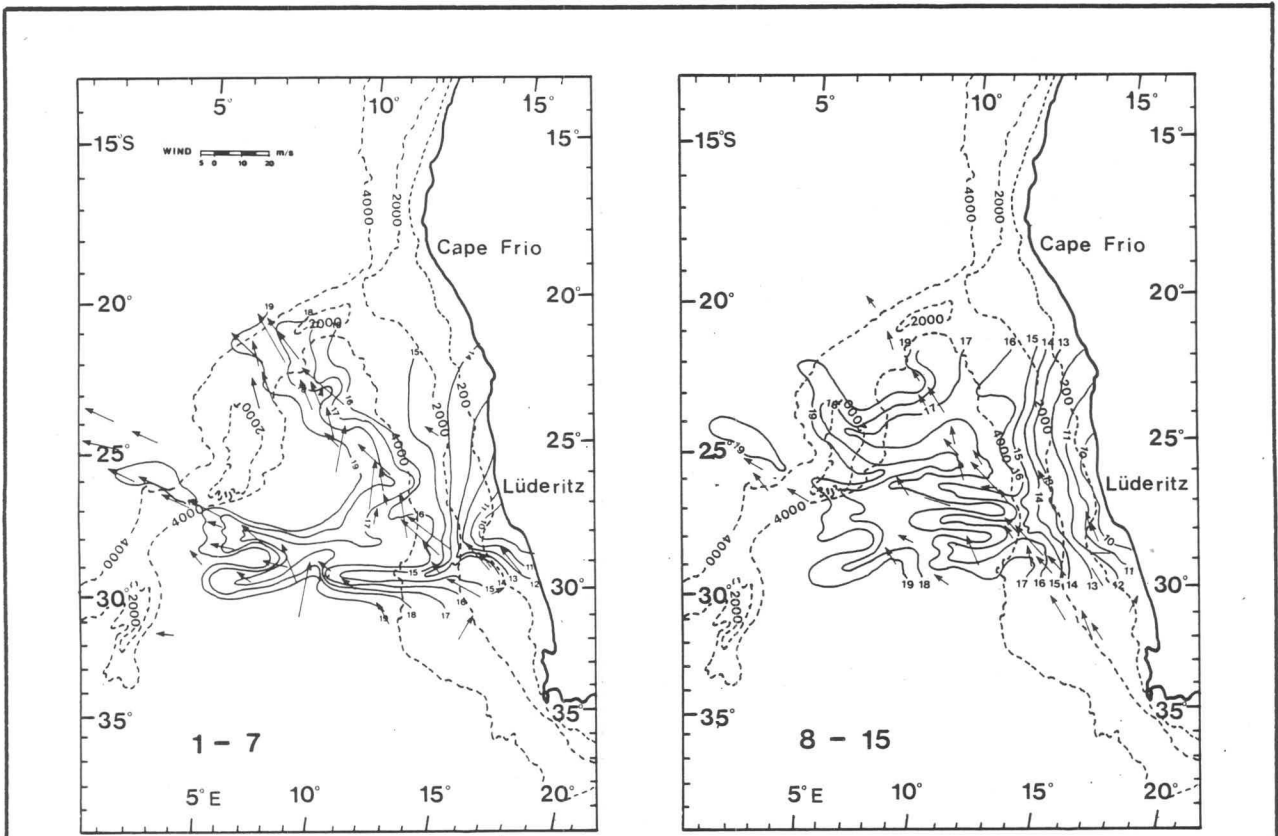
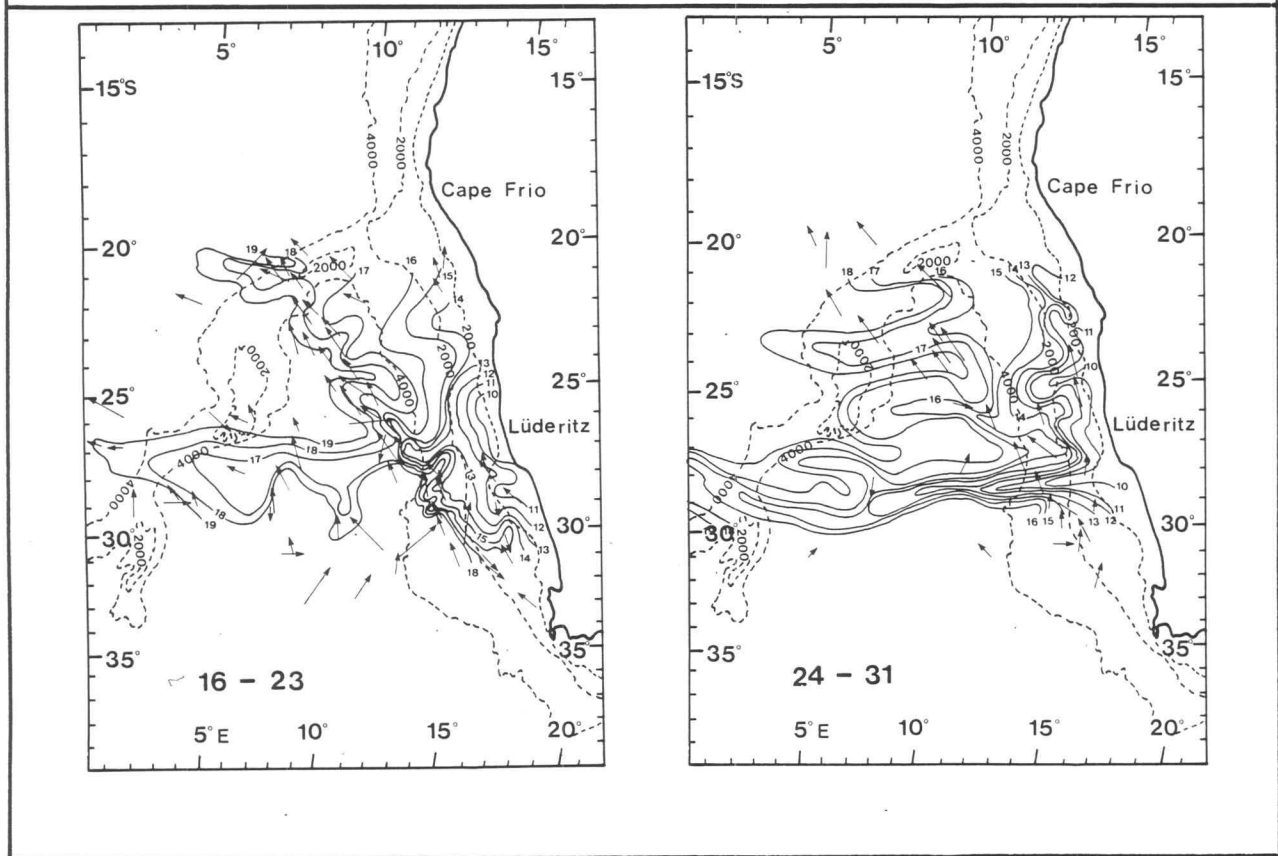


FIGURE 3.5 : Weekly sea surface temperature and wind patterns off the coast of South West Africa during July 1982. The isobaths are given in metres and the sea surface isotherms in degrees Celsius.



temperature gradient. The mean wind direction at the time was  $162^{\circ}$ . For the week of 1 to 7 July mean wind direction was  $143^{\circ}$ , the greatest easterly wind component measured for that month. As the maximum filament length was reached on 13 July it would appear that the reduced wind speeds and lesser easterly wind component were still able to induce filament growth, although not to the same degree as before. An increase in the mean winds during the third week of July to 7.5 m/s saw the restoration of a more intense frontal gradient ( $4^{\circ}\text{C}$  over 50 kilometres) at the root of the filament. This was not associated with renewed filament growth (Figure 3.1) due to the number of westerly and northerly winds that blew at that time (Figure 3.5), giving a mean wind direction of  $191^{\circ}$ . The cross frontal thermal gradient for the rest of the filament remained largely the same as before. The steeper poleward gradient at the root of the filament is seen again. By the end of July the both the magnitude of the mean wind speed and the temperature gradient had changed little from the previous week. An average wind direction of  $169^{\circ}$  resulted in the colder water intruding further along the filament core than before, however.

In consequence, for July 1982 at least, thermal gradients of  $4^{\circ}\text{C}$  to  $5^{\circ}\text{C}$  per 100 kilometres are not uncommon, with some upwelling frontal temperature gradients nearly twice as steep. The general temperatures on either side of the front are about  $13^{\circ}\text{C}$  on the landward side and between  $16^{\circ}\text{C}$  and  $18^{\circ}\text{C}$  on the ocean side. The cross frontal gradient of the outer reaches of the filament are commonly of the order of  $2^{\circ}\text{C}$  to  $3^{\circ}\text{C}$  over 100 to 200 kilometres. How steep the frontal gradient becomes appears to depend on the wind velocity, while the length of the filament is determined by the magnitude of the easterly wind component, which confirms what was found with regard to the effect of berg winds on the distance the filament would intrude into the ocean basin. The ambient ocean temperature beyond the upwelling is about  $20^{\circ}\text{C}$ . The filament extent measured in 1982 was extraordinary, being seen only once in the five years studied. It is not far-fetched to suppose, however, that frontal gradients seen here and in California are not unrealistic portrayals of the frontal temperature gradients to be expected in the smaller filaments seen with such frequency in the upwelling regime.

### 3.3.2 Filament Frequency.

Two of the major upwelling subsystems identified in Chapter Two were used to sample for filament frequency. The coastal strip stretching from Cape Town to  $30^{\circ}\text{S}$  was chosen to represent the southern upwelling zone, while a strip  $5^{\circ}$  to either side of Lüderitz showed the filament activity there. The number of filaments visible each day was counted and shown for those days sufficiently cloud-free to identify and resolve them (Table 3.2).

TABLE 3.2 The average daily filament occurrence for each month for the area between Cape Town and 30°S and the coastal strip 5° of latitude either side of Lüderitz.

Cape Town												
Year	Jan	Feb	Mar	Apr	May	Jun	Jul	Aug	Sep	Oct	Nov	Dec
1979	1.4	1.4	1.4	0.5	1.0	1.2	1.3	0.9	0.7	0.8	0.7	-
1982	1.0	1.7	2.3	1.0	2.0	2.0	2.3	1.2	1.8	2.2	1.4	0.9
1983	0.3	0.2	1.4	1.4	1.1	1.0	0.8	0.4	-	1.3	1.4	0.2
1984	1.3	1.8	1.1	1.1	0.0	0.3	1.3	0.5	0.0	0.3	0.8	0.9
1985	2.0	2.8	1.1	1.6	1.0	1.0	0.8	0.9	0.7	0.8	1.8	2.0
Mean	1.2	1.6	1.5	1.1	1.0	1.1	1.3	0.8	0.8	1.1	1.2	1.0
Lüderitz												
Year	Jan	Feb	Mar	Apr	May	Jun	Jul	Aug	Sep	Oct	Nov	Dec
1979	2.7	1.8	2.0	1.5	0.9	1.7	1.3	0.6	0.8	0.4	1.3	1.9
1982	1.6	1.4	2.1	1.6	1.6	1.7	2.6	1.5	1.7	2.6	2.6	2.0
1983	2.6	1.8	1.7	1.7	2.2	2.5	2.1	2.2	2.4	3.9	1.7	1.5
1984	3.6	1.9	2.1	2.2	1.3	1.1	1.9	0.9	0.5	1.0	1.3	1.4
1985	3.2	3.3	1.7	1.7	1.2	2.3	1.0	0.8	0.9	0.6	1.8	1.7
Mean	2.7	2.0	1.9	1.7	1.4	1.9	1.8	1.2	1.3	1.7	1.7	1.7

The seasonal pattern of filament extent generally reaching a peak in winter off Cape Town (Table 2.1) is contrasted by a weak tendency of decreased filament frequencies during that season (Table 3.2). This is also true of Lüderitz. Although the actual values differ between these two study areas, the monthly frequencies show similar trends. Perhaps the most striking result comes from a comparison of the number of filaments seen for each month with filament extent at Lüderitz for the periods of January to February and December to January. A sharp decrease in the modal upwelling extent (Table 2.1) occurred during those periods; in contrast there was a sharp increase in the number of filaments observed (Table 3.2). This would suggest that the factors involved with filament creation are not necessarily those which facilitate filament growth. There is nothing to suggest that this is also true at Cape Town, however, which indicates some fundamental differences in the upwelling experienced at these two geographic locations. These differences were not only reflected in their size and frequencies but also in the preferred filament tracks of each area.

### 3.3.3 Filament Tracks.

The tracks of the filaments were traced along their stream axes for the entire west coast study area for 1983 to 1985. These tracks were overlaid to show their seasonal locations. During the process of extracting the filament tracks, a predilection for the filament axis of the different upwelling zones to align themselves in a specific direction became evident, particularly off Lüderitz. The overlays of the frontal morphology showed this tendency more clearly and these were used to extract the angles and distances of the filament axes given in Table 3.3.

TABLE 3.3 Orientation and location of the filament axes off Lüderitz. The distances are measured with Lüderitz being a value of 0. Each axis was extended landwards to the 15°E line of longitude. The "+" indicates the distance the extended axes struck this latitude south of Lüderitz, while the unsigned values indicate the distance to the north. The "-" represents those months when the data were insufficient to identify the axis angle or where no apparent axis could be resolved.												
Distance from Lüderitz in kilometres.												
Year	Jan	Feb	Mar	Apr	May	Jun	Jul	Aug	Sep	Oct	Nov	Dec
1978	-	-	-	200	75	250	100	150	175	-	0	125
1979	225	-	25	175	-	125	200	-	-	0	0	-
1982	125	100	0	175	100	50	200	-	-	0	-	175
1983	100	75	150	+50	200	-	100	175	100	150	150	-
1984	-	175	250	175	-	200	300	400	75	-	125	150
1985	0	50	-	-	125	175	100	-	50	-	0	150
Mean	113	100	106	155	125	160	167	242	100	50	55	150
sd	92	54	116	103	54	76	82	138	54	87	76	20
Range	450 km											
Angle of axis in degrees from north.												
Year	Jan	Feb	Mar	Apr	May	Jun	Jul	Aug	Sep	Oct	Nov	Dec
1978	-	-	-	250	212	224	235	245	255	-	252	248
1979	248	-	250	152	-	249	244	-	-	290	277	-
1982	243	254	260	248	249	257	250	-	-	248	-	246
1983	259	261	244	247	235	-	256	245	262	247	247	-
1984	-	236	247	252	-	244	236	236	240	-	250	252
1985	262	245	-	-	237	250	267	-	270	-	279	255
Mean	253	249	250	230	233	245	248	242	257	262	261	250
sd	9	11	7	44	15	13	12	5	13	25	16	4
Range	127°											

Despite the wide fluctuations in observed filament length throughout the month of July, the filament direction and orientation remained constantly directed towards the gap in the Walvis Ridge at 3°E and 27°S. Previous workers (Harris and Shannon 1979) have shown that there is an accelerated stream flowing northwards from the Benguela Current System over the saddle in the Walvis Ridge at 22°S. It would appear that in 1982 the saddle at 27°S induced a similar accelerated flow. The orientation of the Lüderitz filament axes could therefore be related to the macroscale bathymetry.

### 3.4 CONCLUSIONS.

Cross frontal filaments were seen along the entire upwelling zone from Cape Columbine to Cape Frio. On average, the filament sector was 250 km wide with a marked increase to nearly 550 km off Lüderitz (Copenhagen 1953, Parrish et al. 1983). Filaments therefore play an important role in frontal dynamics over the full length of the upwelling regime. The reason for this widespread activity appears to lie in the rapid response of the filaments to changes in the wind field.

Short-term wind events such as the strong land and sea breezes associated with the upwelling zone north of Cape Columbine (Hart and Currie 1960) and the coastal low pressure systems are apparently important factors in filament growth and decay. The rapid surface upwelling filament extent response during berg winds supports this hypothesis. The response of the upwelling front at a more general level is somewhat different, however. This was seen in the 10-day vector analyses. Results from this study showed the lack of influence of the more persistent systems in the determination of the location of the upwelling front offshore at Lüderitz for 1982. It is therefore clear that there must be some other explanation for the sustained growth of the longer filaments. In order to find the explanation, it is suggested that there is merit in investigating mesoscale eddy activity offshore of the upwelling front, should the data become available. An aspect of the physical structure of upwelling filament which does have data is that referring to the temperature structure of filament fronts.

The general frontal temperature gradient is between 0.02°C and .006°C per kilometre at the outer reaches of the filament. This compares well with readings in the Californian upwelling zone. This may vary with any changes in filament activity, but this was not determined.

Filaments are found throughout the year. While there is evidence of a regular seasonal pattern in filament occurrence, both off Cape Town and Lüderitz, it is not very strong. Both of the study areas show relatively similar upwelling frequencies, despite the very dissimilar presentation of the upwelling extent at these two locations. Thus, although the trigger mechanisms responsible for filament creation are present with equal frequency at both locations, the factors responsible for filament growth operate more effectively off Lüderitz than at the Cape. That is, if such growth factors exist in the southern upwelling regime at all. These two areas are not the only areas of preferred filament activity. Outstanding filament zones were also seen off Cape Columbine, Walvis Bay and Cape Frio.

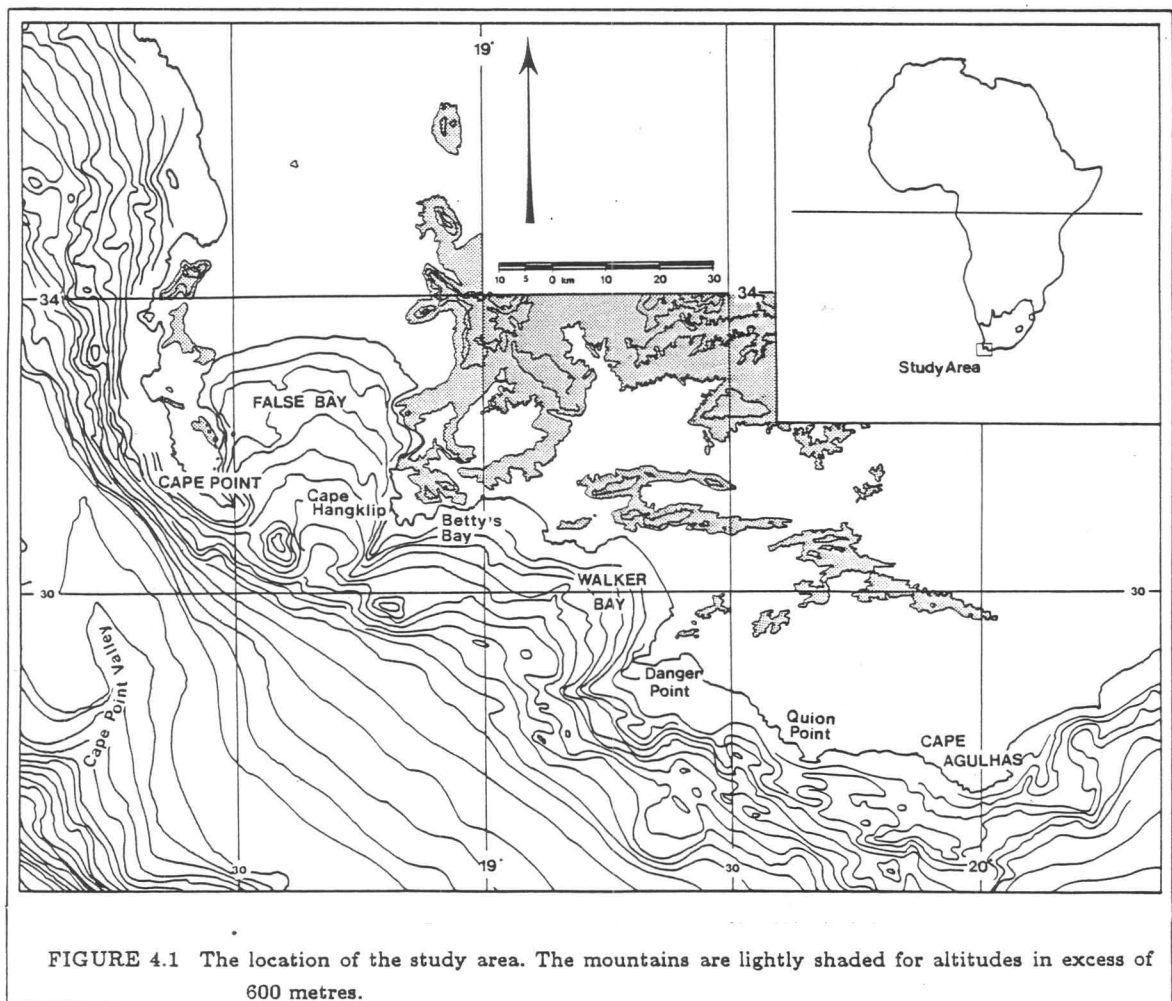
A feature of each group of filaments was the finding of preferred track orientations. At Lüderitz the monthly average angle at which the axis extends offshore varies only between  $230^{\circ}$  and  $262^{\circ}$ . It would therefore seem that these axis angles are generic elements of the upwelling system, possibly determined by the bottom topography. In the case of upwelling filaments at Cape Frio the dominant axis direction follows the Walvis Ridge (Lutjeharms and Stockton 1987). Those at Lüderitz are apparently aligned to flow through a gap in the Walvis Ridge. While this is almost certainly the case of the cold water stream seen in 1982, preferred orientation of the plume axis angles of Table 3.3 suggests that this is probably true of most of the filaments in the Lüderitz upwelling area.

While the changes in filament frequency seen at Cape Town and Lüderitz display similarities, some important differences have been reported. One such difference is that of maximum upwelling extent. Therefore, the factors operating on the upwelling in each of these areas may be fundamentally different. These factors, as they effect the upwelling of the capes will now be addressed in Chapter 4.

## CHAPTER FOUR

### SOUTHERN CAPE UPWELLING

The southwestern Cape coastal zone between Cape Point and Cape Agulhas (Figure 4.1) forms the western boundary of the important pelagic fish spawning ground on the Agulhas Bank. Pilchard and anchovy larvae use this area as a nursery before moving westwards to stock the Benguela upwelling system (Boyd et al. 1985). It is not surprising, therefore, that this area has been the subject of much study. The majority of these studies cover the temporal scale of the order of hours to a few weeks and at a spatial scale of a few kilometres (Shannon et al. 1981, Schumann et al. 1982, Boyd et al. 1985, Nelson 1985, Jury 1985, Jury 1988). While filaments dominate and studies of them are important for a full understanding of the upwelling of this region, it is suggested that they may not be the only form that upwelling takes. Furthermore, as pelagic spawning conditions vary considerably throughout the year as a result of seasonal weather changes (Boyd et al. 1985), more general and longer term studies are needed of this region. Consequently a wider understanding of the overall upwelling regime around the southern Cape coast is required to complement what is already known about cape filaments.



#### 4.1 ANATOMY OF A CAPE FILAMENT.

The upwelling filaments streaming from the capes between Cape Point and Cape Agulhas are shallow occurrences. They do not extend deeper than 100 to 200 metres and as result respond very rapidly to changes in the winds (Taunton-Clark 1985). Furthermore, unlike that of deep-sea filaments, the morphology of cape filaments can be directly related to the sea bottom topography.

In the shallow inshore water the Ekman divergence responsible for upwelling cannot develop fully. Therefore, instead of an offshore movement of the surface required for upwelling (Figure 1.3), a longshore current results. This current flowing parallel to the coast, or in the shallower parts even drifting onshore, does not result in upwelling; on the contrary, in the case of onshore flow, it may give rise to localised downwelling, particularly in the bays (Schumann et al. 1982). On the seaward side of the bays, where the water is deeper, a more strongly developed Ekman divergent flow is possible. A slight offshore component to the surface flow can result. If strong enough the flow may initiate weak upwelling. However, should the longshore current be forced around a cape, Bernoulli acceleration of the stream will take place (Nelson and Hutchings 1983, Jury 1985). Under these circumstances the vicinity of the cape becomes a zone of surface divergence (Schumann et al. 1982). Upwelling is probable under such conditions. In turn, a near surface jet induced by the thermal contrast between the cooler upwelled water and the ambient may develop (Bang 1971, Nelson and Polito 1987). As a consequence, the upwelling will appear to start at the cape and then progress in alignment with the direction of the prevailing wind (Schumann et al. 1982). It is clear, therefore, that the distinctive morphology and location of the southern Cape upwelling filaments are directly controlled by the bathymetry off the coast of the area.

#### 4.2 PHYSICAL FACTORS IN CAPE UPWELLING.

##### 4.2.1 Bathymetry.

As far as Cape Point and Cape Columbine are concerned, the bathymetry is responsible for the supply of the cold bottom water that upwells to the surface. The pathway for this cold water found in the Cape Point filament is the Cape Point Valley incised onto the steep inner continental slope. (Shannon et al. 1981, Jury et al. 1985). During spring, cold water flows over the shelf from the west, remaining there until autumn and upwelling of Central Water can occur close inshore west of Cape Agulhas (Shannon 1985).

The Agulhas Bank is the dominating bathymetric feature at the south of the continent. It is a broad piece of the continental shelf extending about 250 kilometres offshore (Figure 1.2). The warm Agulhas Current follows the eastern edge of the Agulhas Bank, while the stretch of coast between Cape Point and Cape Agulhas forms the northern margin. Along this margin five significant headlands are found. Starting with Cape Agulhas in the east and progressing westwards there are Quoin Point, Danger Point, Cape Hangklip and Cape Point (Figure 4.1). Each of these capes is large enough to induce filament activity under the right circumstances. Just how the filaments react once formed depends not only on the bathymetry but also on the winds; winds which are significantly modified by the coastal topography (Jury 1985).

#### 4.2.2 Coastal Topography.

The mountains found along the coast obstruct the equatorward summer winds to a greater or lesser extent, depending on the depth of the wind system and the topographic magnitude (Jury 1985). Mountain elevation differs considerably along this coast. It exceeds 1000 metres along the Cape Peninsula spine, falling to less than 100 metres at Cape Agulhas (Figure 4.1). This is important, particularly in summer when the southwesterly winds are capped by a shallow inversion. The inversion effectively confines the airstreams to heights below the crests of the higher mountains (Jury 1985). It follows that a wind system capped by an inversion layer of about 800 metres will be affected differently at Cape point than at Cape Agulhas (Jury 1988). In the event of a low level inversion, the airstream rounding a cape, as in the case of Cape Point or Cape Hangklip, is subject to Bernoulli compression and acceleration similar to that seen in the longshore drift (Jury 1988). As the shallow wind streamlines are compressed by the mountains and acceleration takes place, wind shear induces an element of cyclonic vorticity to the airstream (Jury 1985). The resulting Cape Point and Cape Hangklip upwelling filaments show the effects of this by generally flowing along a northwesterly track. During winter the topography plays a less important part because of the increased depth of the westerly winds (Jury 1988).

In addition to the height of the mountains, their topographic alignment is also of important in modifying the low-level winds (Jury 1988). The Kleinrivier mountain range along the Walker Bay coastline is oriented west to east, while the Table Mountain group lies along a north to south axis (Figure 4.1). These axes serve to align most of the wind fields over the adjacent ocean almost parallel to the coast (Jury 1985). As a result any wind with a southeasterly component becomes favourable for upwelling in the area between Cape Point and Cape Agulhas. The southeaster is the prevailing summer wind

over the southwestern Cape as they blow around the macroscale pressure system in the South-Eastern Atlantic Ocean.

#### **4.2.3 Influential Wind Systems.**

##### **4.2.3.1 Macroscale Winds.**

As a result of seasonal migration of the macroscale high pressure cell, the major upwelling season is considered to be in summer (Boyd et al. 1985). This is related to the South Atlantic Anticyclone (SAA). Kamstra (1985) found that, if the (SAA) over the South-East Atlantic Ocean became well established with a continental heat low over the Southern African subcontinent, a strong zonal pressure gradient would result. Strong south easterly winds would result. This is important since Schumann et al. (1982) reported no cape upwelling without an easterly component to the winds. Furthermore, according to Schell (1970) strong southeasterlies caused intense upwelling south of about 30°S from depths of 350–400 metres or more. As these isobaths are found about 35 kilometres out to sea, Schell's (1970) findings suggest that the upwelling seen off the southern Cape coastline need not necessarily take the form of a filament. Whatever form the upwelling takes, it is subject to the vagaries of the wind.

##### **4.2.3.2 Mesoscale winds.**

As is the case at Lüderitz, the southern upwelling zone is subject to land/sea breezes and passing coastal lows. Unlike the position at Lüderitz, however, the upwelling in the south is subject to changes in surface winds caused by a high pressure event, known as the bud-off high, which forms a ridge of high pressure to the south of the continent.

##### **4.2.3.3 Bud-Off Highs**

The prevailing seasonal wind pattern is modified periodically by bud-off high pressure cells moving eastwards along the south coast. This high pressure system, or bud-off high, ridging in produces shallow winds with the necessary easterly component which are particularly conducive to upwelling off Cape Hangklip and Cape Point (Jury 1985) and possibly also off Danger Point (Jury 1988). Apart from the bud-off highs, another influential mesoscale weather system is the easterly moving cyclone. These are low pressure systems forming ahead of the planetary waves in the subtropical jetstream which are steered by the SAA.

#### 4.2.3.4 Temperate Cyclones

During summer such low pressure cells move well south of the SAA and introduce a periodic acceleration of winds favourable to upwelling (Nelson 1985). During winter the cyclonic systems move along a track far north of that followed in summer and cause periodic northwesterlies along the coast. In between these events strong southerly winds blow in the region of Cape Point (Nelson 1985). Such winds are favourable to upwelling there. Upwelling does not result from these winds at the headlands eastwards of Cape Point, therefore a stronger seasonal aspect to upwelling occurrence would be expected at those capes than at Cape Point (Figure 4.2).

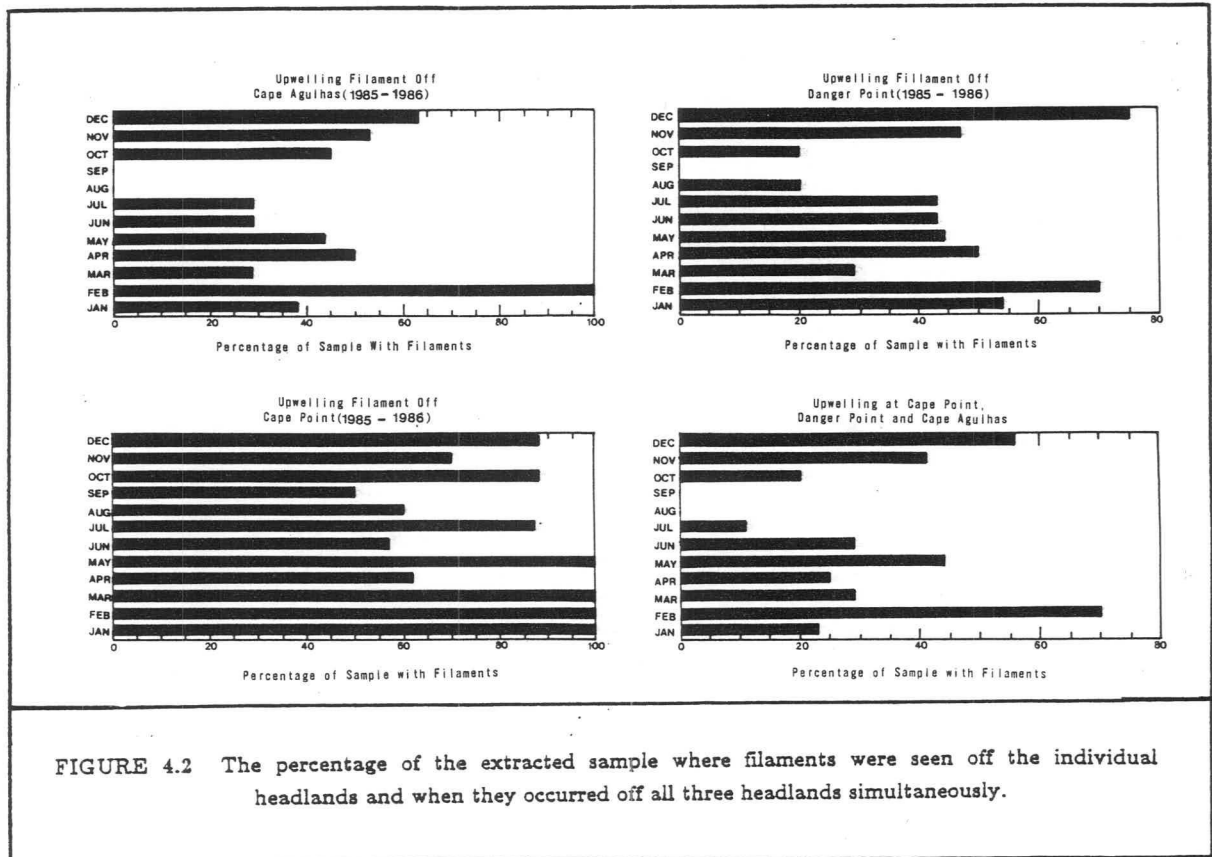
In the winter months the northward shift of the SAA allows the low pressure perturbations to affect the southern tip of Africa, producing westerly to northwesterly winds (Taljaard 1972, Schulze 1974). These winds, if severe, thoroughly mix the water column over which they blow (Schell 1970, Kamstra 1985, Boyd et al. 1985). This mixing process serves to suppress either the upwelling or the surface expression of the upwelling along the southern coastal area between Cape Point and Cape Agulhas during winter, making it difficult to distinguish it in satellite infrared imagery.

#### 4.3 DETERMINATION OF FILAMENT ACTIVITY.

With use of the infrared satellite images for 1984, 1985 and 1986, any cold water stream originating at one of the three major headlands of Cape Point, Danger Point or Cape Agulhas was noted for every day the required stretch of the sea surface was visible. These were graphed for each headland separately and severally for each month (Figure 4.2). Here the tendency for reduced winter upwelling activity is clear at Danger Point and at Cape Agulhas. As previously suggested, the seasonal pattern at Cape Point is not as clearly defined. For example, the Cape Point filament was present during March with a much greater frequency than at Cape Agulhas or Danger Point. Furthermore, the total lack of upwelling at the last two locations during September is only partially reflected by a reduction of upwelling at Cape Point so the seasonal upwelling at Cape Point is not as marked as it is at the headlands to the east.

From the above discussion it is clear that the knowledge about filaments as they occur around capes is comprehensive. There is inadequate documentation, however, of seasonal patterns of the upwelling in more general terms. The term "more general" is used here in the sense of looking at the upwelling phenomenon as a whole and not as four independent upwelling inducing units. As the break in coastal orientation at Cape Point





clearly divides the southern upwelling into two, the headlands to the north of Cape Point were not considered.

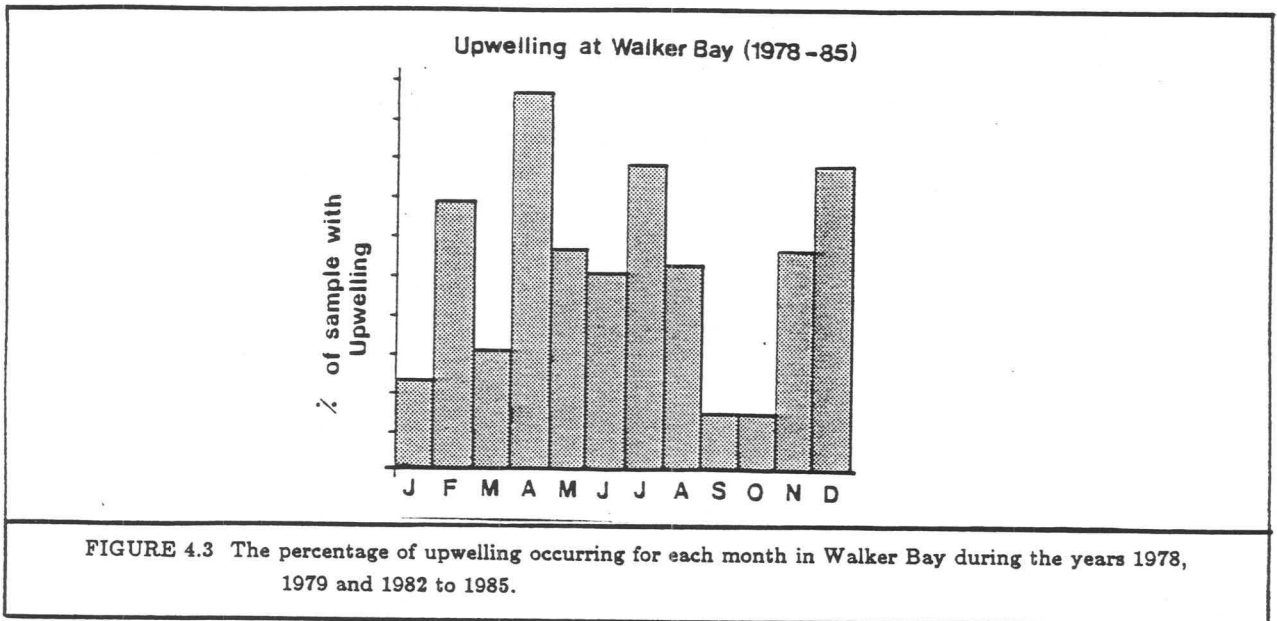
#### 4.4 GENERAL UPWELLING REGIME.

In order to determine the general upwelling as well gaining an idea of the surface area of upwelled water adjacent to the coastal stretch between Cape Point and Cape Agulhas, an arbitrary central point was plotted in the middle of Walker Bay. An initial step was an elementary "present or absent" analysis for daily upwelling in the bay. The results are summarised for each month in (Figure 4.3). In this figure the percentage of upwelling events that occurred within the combined total cloud-free data set available for each month over the entire sampling period has been graphically represented.

The monthly upwelling at Walker Bay shows that the modal upwelling month is not in summer (Figure 4.3) as has been suggested by Boyd et al. (1985) but in early autumn. The April maximum is preceded by a lull in March. The situation in the winter is somewhat more complex because the well mixed Agulhas Bank waters tend to show an even sea surface temperature, with the greatest grey scale contrast occurring along the



Agulhas Current margin. This analysis was insufficient to give an indication of the areal extent of the cold water body. As a result, additional measurements were made.



#### 4.4.1 Meridional and Zonal Extent of Upwelling.

These additional measurements enabled the extent of the zonal and meridional upwelling to be estimated by measuring the distance of the most westerly, southerly and easterly contiguous upwelling from the point in the centre in Walker Bay that was used previously.

Not surprisingly, the westward extent was usually the greatest. As already seen in Table 2.1, upwelling plumes extended about 40 kilometres beyond Cape Point as a rule. The longest filament measured in February 1984, extended about 200 kilometres beyond Cape Point. This filament, as do many others streaming off Cape Point terminated in a characteristic cyclonic eddy (Stockton and Lutjeharms 1988). The mean southerly extent was about 20 kilometres, which lies opposite Danger Point. It would be reasonable to accept that a filament from this cape acts as a thermal barrier which may inhibit the upwelling in Walker Bay from routinely spreading onto the Agulhas Bank. Nonetheless, upwelling did stretch beyond this barrier. In fact, on 22% of the occasions when measurements could be taken, the upwelling reached as far as 37,5 kilometres offshore at Walker Bay. At this distance the upwelling front lies roughly over the 200 metre isobath. These fronts would overlies the poleward jet measured by Nelson and Polito (1987) should they in fact exist that far east. It is interesting to note that 80% of these extensive events occurred in the months between April to July, as did the biggest upwelling extent. In June 1985 the upwelling front was measured about 75 kilometres south of Walker Bay. To the east, Cape Agulhas was the most consistent point at which the upwelling ceased. One episode was measured where the contiguous upwelling extended to



Cape Infanta, about 60 kilometres east of Cape Agulhas. This episode also occurred in winter. In general, therefore, the zonal extent of the upwelling regime between Cape Point and Cape Agulhas is confined to the sea inshore of the 200 metre isobath. Meridional boundaries are also fairly well defined. The eastern boundary is at Cape Agulhas, while the western extension is usually at the end of a filament about 40 kilometres beyond Cape Point.

During the course of the measurement of upwelling it became apparent that at this spatial resolution three recurring upwelling patterns could be identified.

#### 4.5 RECURRING UPWELLING PATTERNS.

The first, least frequent pattern consists of well-developed upwelling off the Cape Peninsula and further north along the coast but with no recognisable upwelling between Cape Point and Cape Agulhas (Figure 4.4). This example, shows extensive upwelling was evident from Cape Point to Cape Columbine. Off these two headlands the extensive upwelling filaments extend more than 100 km seawards, ending in cyclonic eddies. Warmer surface water of Agulhas origin (Catzel and Lutjeharms 1987) may be seen just offshore of the upwelling front and in some cases being drawn in by the frontal eddies. The upwelling terminates quite sharply at Cape Point. There is no surface evidence of any upwelling between Cape Point and Cape Agulhas in this case.

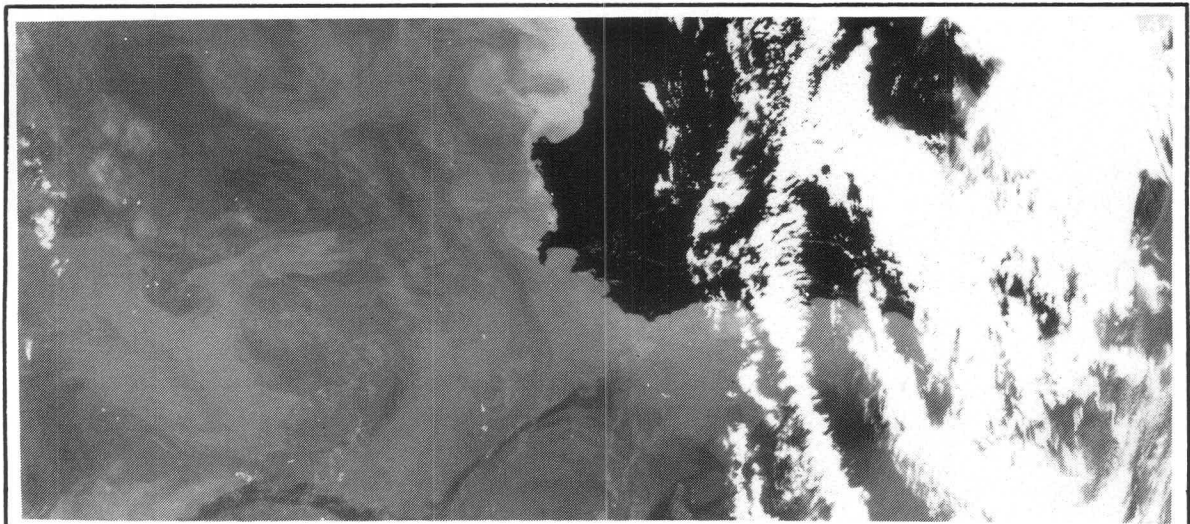


FIGURE 4.4 A well mixed water body over the Agulhas Bank for 26 September 1986. The thermal infrared image is from the NOAA-9 satellite. The lighter shades indicate lower sea surface temperatures. This sea surface temperature pattern is typical of the winter regime.

The second pattern is one of well-developed upwelling cells at the main headlands, usually with extensive seaward filaments (Figure 4.5). Well-developed upwelling prevails at Cape Point and Cape Columbine. However, Cape Agulhas, Danger Point and Cape

Hangklip also exhibit intense upwelling. Of particular interest is the filament from Cape Hangklip which extends across the mouth to False Bay. Some colder surface water seems to be entering False Bay along its western shore. The significance of this upwelling mode, which is representative of a small but consequential period of each year, lies in the observation that the upwelling along the coast of the west Agulhas Bank is not continuous but occurs in distinct cells related to the three mainlands; neither is it contiguous with the upwelling north of Cape Point.

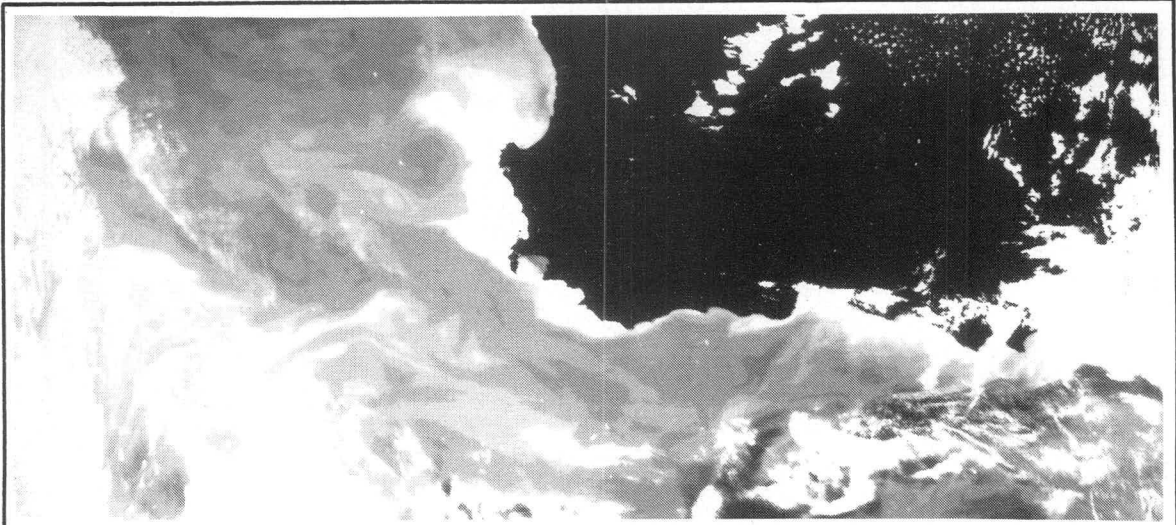


FIGURE 4.5 Characteristic upwelling mode as it appears along Southern Africa's south western Cape Coast for 12 December 1986. Typical summer cape induced filaments are being advected from Cape Agulhas, Cape Hangklip, Cape Point.

The third mode has extensive, contiguous upwelling from Cape Agulhas northward along the whole western coast (Figure 4.6). This is the most frequent upwelling pattern. During such extensive events there may be upwelling at the headlands to the east of Cape Agulhas (Schumann et al. 1982).

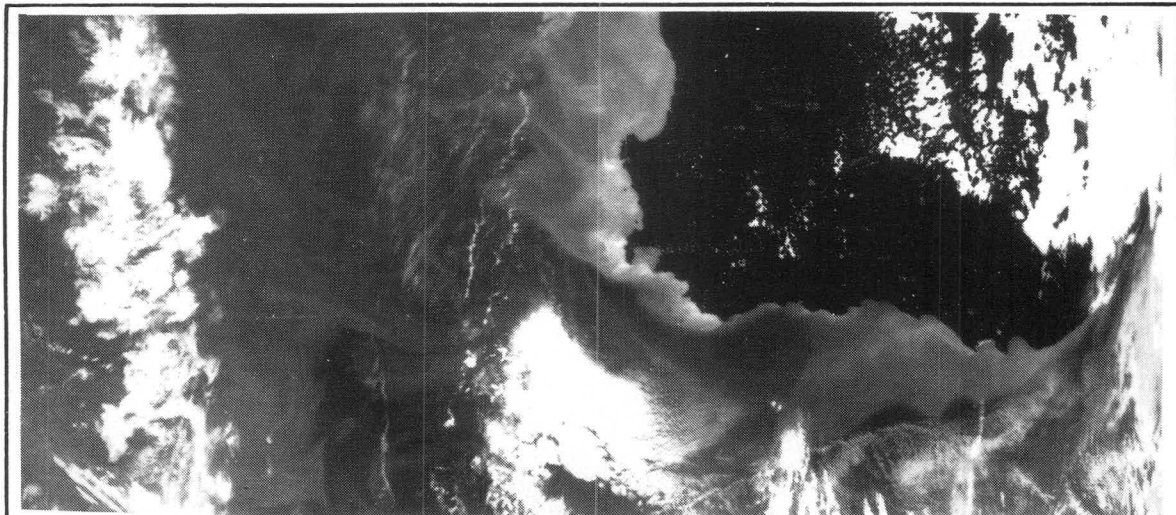


FIGURE 4.6 Image of a typical summer upwelling pattern between Cape Point and Cape Agulhas for 6 February 1986. Although the upwelling is apparently influenced by the capes, it is not necessarily in the form of well developed filaments, but forms a contiguous cold water mass of some extent.

Considering that the second mode of upwelling conforms to the cape filament upwelling regime most commonly described, only case studies highlighting the first and third upwelling patterns are offered here.

#### 4.5.1 Case Studies.

##### 4.5.1.1 Non-Upwelling Conditions

###### 4.5.1.1.1 January, 1982.

As the wind measured at Cape Point is considered to differ so fundamentally from that at Cape Agulhas (Jury 1985), the winds for both of these stations have been considered. Thus wind run for the month of January, 1982 as measured at the Cape Point and Cape Agulhas lighthouses are given in Figure 4.7. There was no upwelling during this summer month in Walker Bay. This was as a result of the southwesterly and southerly winds, unfavourable to upwelling (Schumann et al. 1982), that predominated during the first 12 days of the month. These winds resulted from a high pressure cell situated to the southwest of Cape Point. The southeasterly wind that blew from 12 January to 14 January when a weak high pressure cell ridged in to the south of the continent was unable to exert sufficient surface wind stress on the water to induce any upwelling before the southwest winds resumed again. This was also true of the winds associated with the coastal low pressure system of 15 January. It was not until January 26 that a significant easterly component was introduced into the wind regime. Unfortunately extensive cloud cover prevented further analysis.

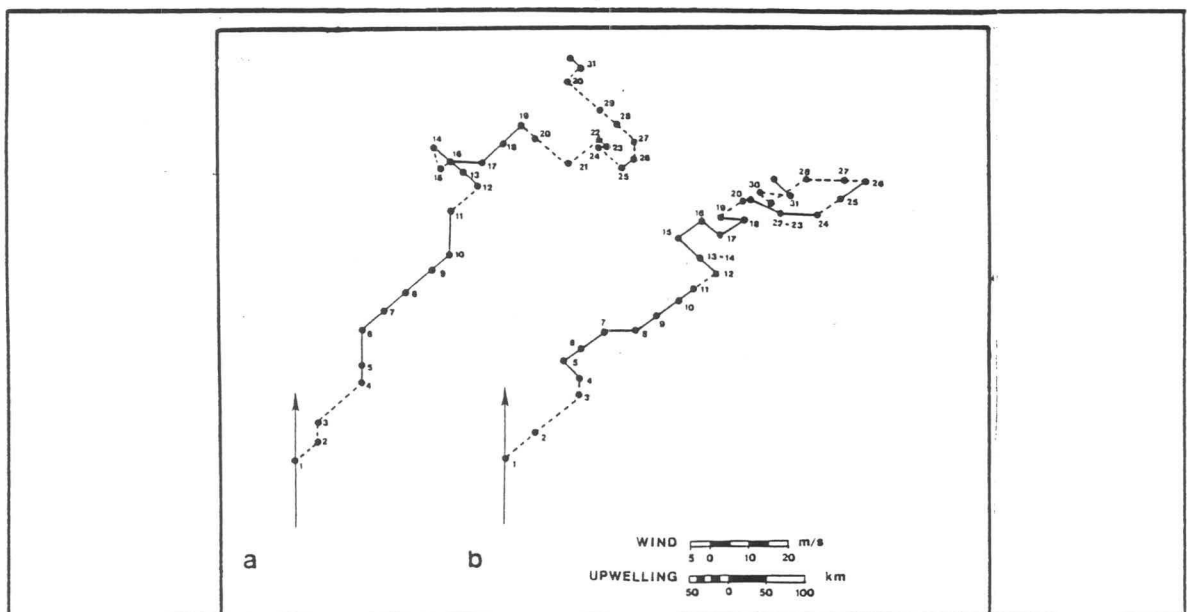


FIGURE 4.7 The 14h00 wind-run as recorded at Cape Point (a) and Cape Agulhas (b) for January, 1982. The solid lines represent those days for which suitable satellite imagery was available. There was no upwelling between Cape Point and Cape Agulhas over this period.

## 4.5.1.1.2 July, 1985

During this winter period the winds measured by the Cape Agulhas (Figure 4.8) lighthouse differed markedly from those of Cape Point. This latter station reported extremely variable winds and the thorough mixing of the Agulhas Bank waters as suggested by Schell (1970) is evident from the satellite imagery. The west winds predominating at Cape Agulhas served to mix the water up the east coast to Port Elizabeth. As a result of this extensive mixing of the cooler subsurface and the shelf surface waters, the line of greatest contrast, which would normally indicate the upwelling frontal zone, occurred along the northern margins of the Agulhas Current as it moved around the steeply sloping Agulhas Bank shelf. The picture remained essentially the same as that seen in July for August 1985.

As a result of this, as Schumann et al. (1982) found, without an easterly component to the wind direction, upwelling will not arise. Furthermore, the easterly winds must apparently exceed some undetermined threshold velocity and/or duration to induce upwelling. This can be deduced from the lack of upwelling during January 1982 despite southeasterly winds blowing for a period longer than 48 hours at Cape Point (Figure 4.7). This velocity was clearly exceeded either before, or during January and February 1984.

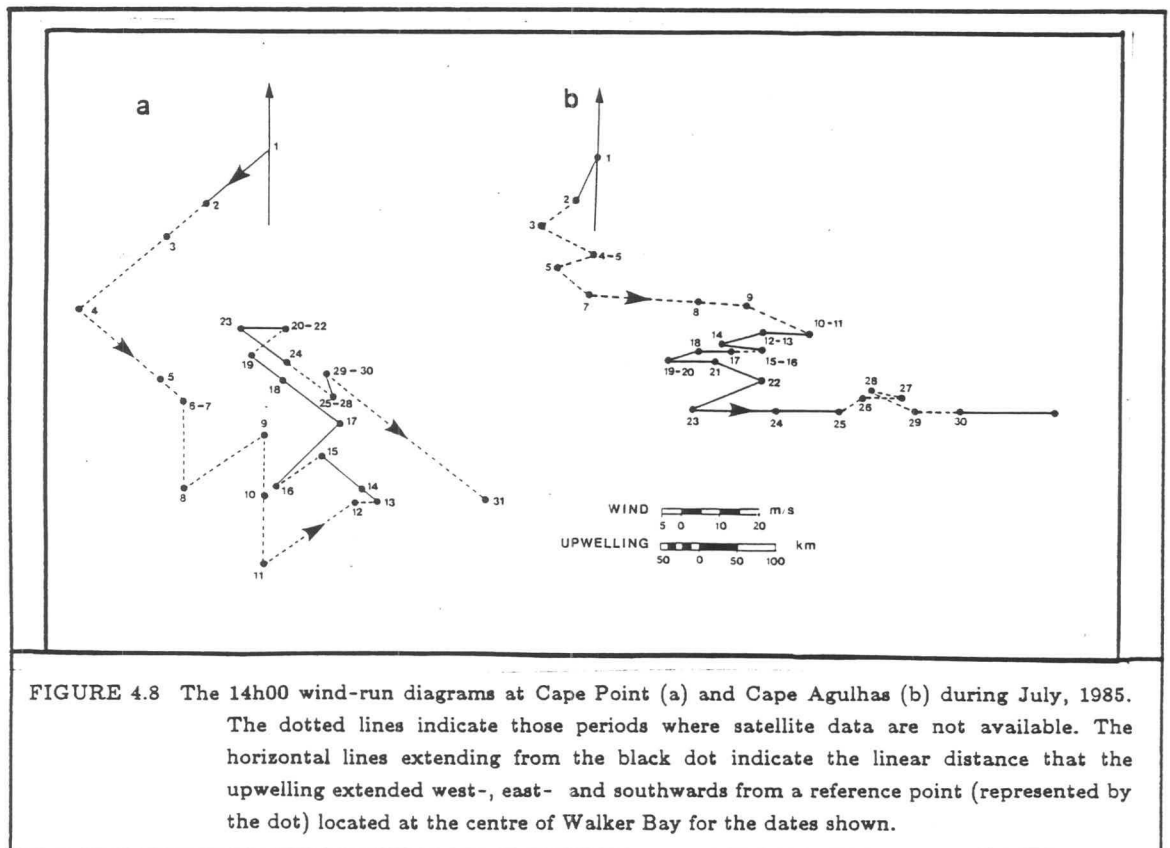


FIGURE 4.8 The 14h00 wind-run diagrams at Cape Point (a) and Cape Agulhas (b) during July, 1985. The dotted lines indicate those periods where satellite data are not available. The horizontal lines extending from the black dot indicate the linear distance that the upwelling extended west-, east- and southwards from a reference point (represented by the dot) located at the centre of Walker Bay for the dates shown.

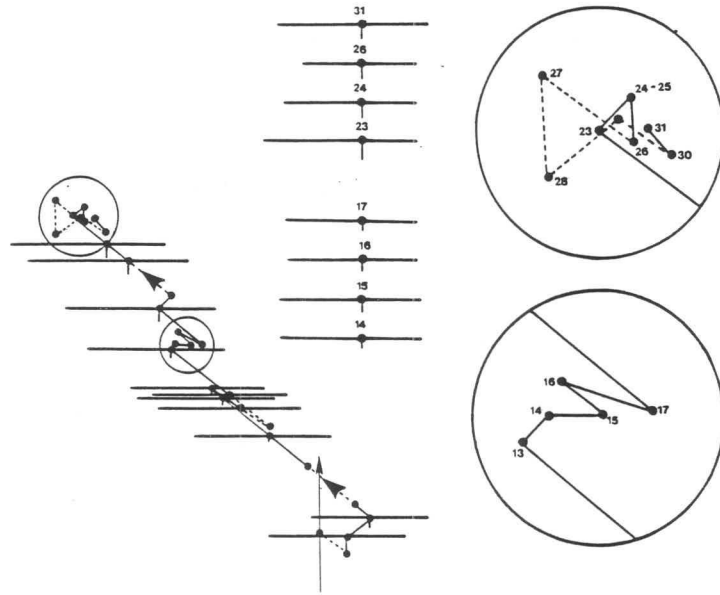


FIGURE 4.9 The 14h00 wind-run diagrams from Cape Point during January 1984. The dotted lines indicate those periods where satellite data are not available. The horizontal lines extending from the black dot indicate the linear distance that the upwelling extended west-, east- and southwards from a reference point (represented by the dot) located at the centre of Walker Bay for the dates shown.

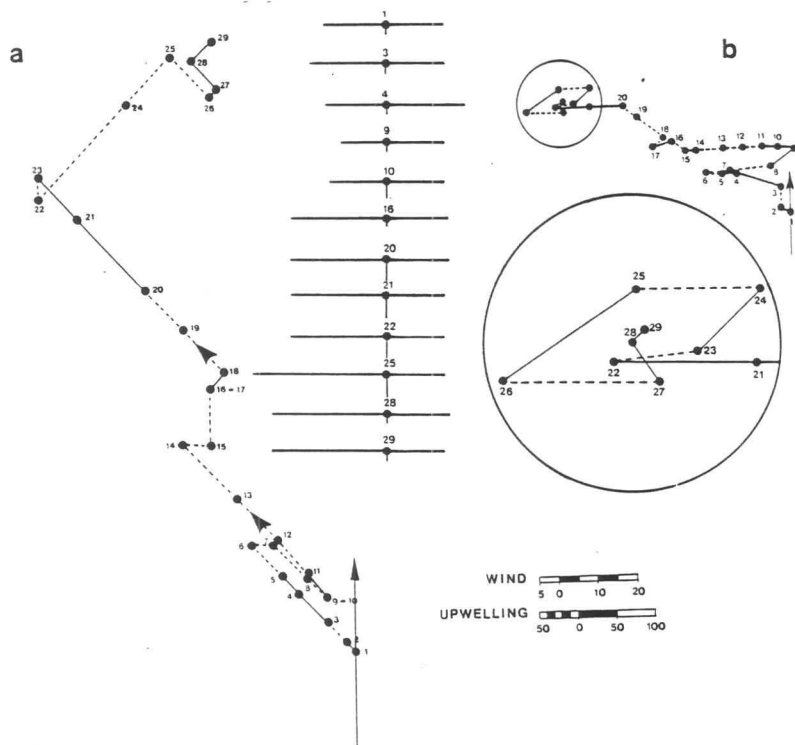
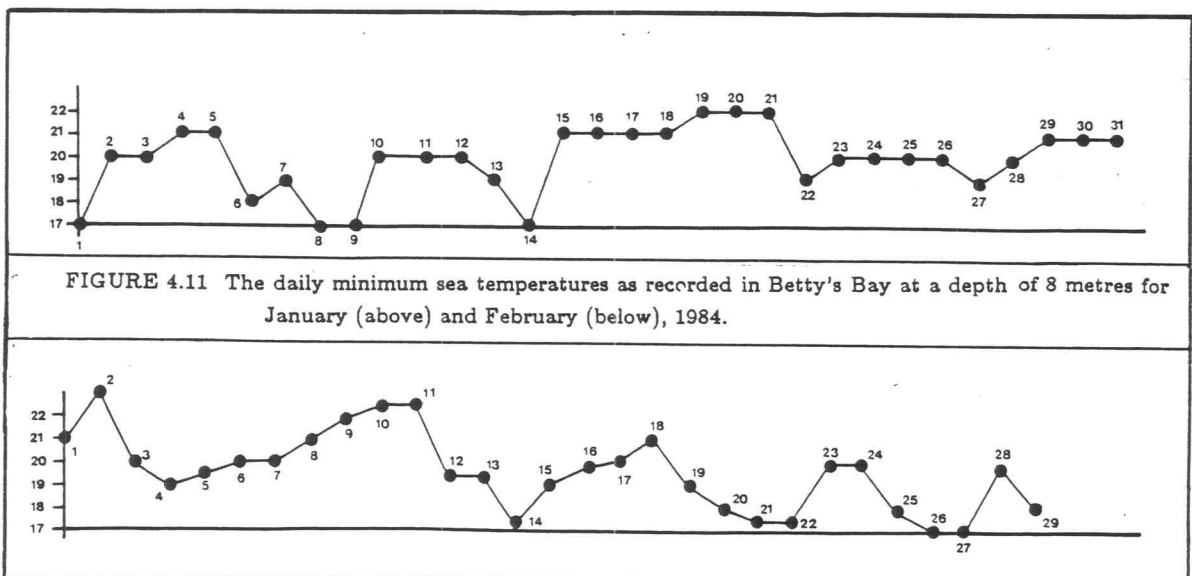


FIGURE 4.10 The 14h00 wind-run diagrams from Cape Point (a) and Cape Agulhas (b) during February 1984. The dotted lines indicate those periods where satellite data are not available. The horizontal lines extending from the black dot indicate the linear distance that the upwelling extended west-, east- and southwards from a reference point (represented by the dot) located at the centre of Walker Bay for the dates shown.

#### 4.5.1.2 Extensive Zonal Upwelling

##### 4.5.1.2.1 January and February, 1984.

The southeasterly winds predominated during these two summer months (Figures 4.9 and 4.10). The greater easterly wind component than that seen in the previous case studies was evidently the major upwelling driving force. Plumes extend eastwards for some distance off Cape Point and Cape Agulhas. The southerly wind component probably acted to counter any great extension of the upwelling northwards onto the Bank. The Weather Bureau synoptic charts for this period show a preponderance of high pressure systems, described by Jury (1985) as being particularly effective in inducing cape filaments, ridging in to the south of the country. The passage of the coastal lows around the coast on the dates of 3, 8 - 9 and 14 - 15 January had no noticeable influence on the sea surface temperature distributions. This may be due to a two-day lag between the wind forcing and any upwelling response along this coast (Boyd pers comm.). It is interesting that at an automatic electronic temperature sensor situated at a depth of 8 metres in Betty's Bay the temperature dropped 3°C during the passage of the coastal low (Figure 4.11). Whether these temperature fluctuations were due to upwelling, is not clear, however. Five days of constant south easterly winds are also clearly reflected in these data. On the other hand, erratic winds reduced the westward extent of the upwelling from Walker Bay by about 200 kilometres over a 24-hour period (Figure 4.10). The eastward extent of the upwelling was reduced by 25 kilometres over the same time. These fluctuations were noticeable in the data from both the satellite imagery and Betty's Bay sensors. This decay was continued with two westward moving cyclonic systems between 6 and 9 February (Figure 4.10). Ridging high pressure systems then became dominant and the upwelling became strongly reactivated for the rest of the month.



Apart from the now clear need for easterly winds, this case study shows another characteristic of the filaments. Despite being apparently well developed, the upwelling appeared to be singularly fragile. With a short-term loss of favourable wind stress the filaments contracted very rapidly. It might well be that the longer the filament grows the more sensitive it becomes to the removal of upwelling positive wind stress. This could be accounted for by the reduction in the effect of the Bernoulli acceleration on both the wind and the water streams around the capes with increasing distance.

#### 4.6 CONCLUSIONS.

In comparison to the deep-sea filaments off Lüderitz, there is a greater understanding of the short-term filament dynamics around the various capes found in the southern Cape study area. This may be attributable in part to the relative confines within which the cape upwelling is found. If one considers only the coast between Cape Point and Cape Agulhas, when upwelling does occur it rarely exceeds a meridional extent of 40 kilometres from the coast at Walker Bay. The average distance that the front occurs south of Walker Bay is exactly half of that. To the west the upwelling can extend as much as 200 kilometres beyond Cape Point. The norm is about 40 kilometres, however. Cape Agulhas is the effective eastern boundary of any regular upwelling.

This may also be the reason why the influence of the winds on the upwelling is also well documented too. Easterly winds are clearly the key to the initiation of any upwelling. What is not clear, however, is the threshold wind velocity or favourable wind duration required for any upwelling. Once initiated, the upwelling filaments are apparently sustained as long as the easterly wind is active. The more extensive the filament becomes, however, the more rapidly they contract during relatively short periods of unfavourable winds. Two reasons for the restricted filament length could be suggested. Firstly, where any northward moving current passing close to the Cape Point may truncate the filaments or alternatively induce the cyclonic vorticity so regularly seen off Cape Point on satellite imagery (Stockton and Lutjeharms 1988). Such a flow may take the form of an offshoot of the Agulhas Current sometimes seen advecting warm water northwards just offshore of the upwelling front (Catzel and Lutjeharms 1987). The second reason might be some inherent driving force operating within the deep sea filaments that is absent in cape filaments. The solution may well be a mixture of both situations. However, whatever the reasons for limited filament length, the longer filaments formed at the capes east of Cape Point are readily eroded by adverse winds and may fade away completely. This situation is one of the three recurring upwelling modes identified.

From the wide range of upwelling scenarios seen in the study area three basic sea surface temperature patterns were described:

- i) upwelling north of Cape Point, not between Cape Point and Cape Agulhas;
- ii) upwelling filaments at all at the capes;
- iii) full extensive and contiguous upwelling along the whole coast.

Although the record is limited, it would be plausible to suggest that the upwelling regime may well go through a cycle, starting with the first mode, progressing through the second into the fully developed upwelling of the third. As noted earlier the upwelling may then become unstable and be easily eroded once it becomes too extensive. This sequence might possibly result from the three to six day temperate cyclone induced cycle to the southernwestern Cape upwelling (Nelson 1985).

## CHAPTER FIVE

### SUMMARY and CONCLUSIONS

Each infrared satellite image used gives a synoptic snapshot of the eddies, filaments and convolutions within the Benguela Upwelling system at a given time. The complexity of the patterns present the researcher with a surfeit of visual data. Using relatively simple graphic procedures the data can be reduced to reveal much that is new about the nature of the upwelling front, as well as corroborating a great deal that was previously hypothesised. This was only possible due to availability of the comprehensive library of daily satellite imagery over a six year period at the CSIR in Stellenbosch. This lengthy data record allowed more general statements to be made as to the annual fluctuations of the upwelling, as well as more clearly defining any seasonal trends. On the other hand the daily Meteosat imagery gave valuable insights into the day-to-day perturbations at the upwelling front. Another feature of the satellite imagery used was the extensive coverage they offered, extending over an area from Cape Frio to Cape Agulhas. Furthermore, when using both Meteosat and NOAA imagery the spatial resolution was fine enough to study the two main upwelling zones identified separately. The first zone studied stretched between Cape Frio and Cape Columbine, while the second concentrated on the coast between Cape Point and Cape Agulhas. Particularly when studying the southwestern Cape coast it was important to be able to see the mesoscale features as well as those at the macroscale.

The ability to see the sea surface at a variety of scales was necessary as cross-frontal extrusions into the ocean basins and intrusions into the upwelling regime comes in a wide range of sizes. At the macroscale two upwelling zones were identified. The first is the upwelling core along the coast which exhibited well-developed and persistent upwelling. Offshore of this is an area in which more transient filament activity predominates. This outer zone is one of constant change and presents highly variable frontal boundary locations.

The northern boundary closely approximates that suggested by Shannon (1985) of 17°S. Cape Agulhas was the effective southern boundary of any regular upwelling. The mean

offshore extent of the outer upwelling is 270 kilometres off Lüderitz and 45 kilometres off Cape Town.

The trends in seasonal changes in the distance offshore of the front offer some confirmation of, as well as some contradictions to, previous findings. The winter maximum in frontal extent at Lüderitz is in agreement that reported by Shannon (1985). The similar situation for Cape Town is at odds with the findings of Nelson (1985) and Boyd et al. (1985) who documented a summer maximum for this upwelling zone. Although the winter upwelling extent is the greater of the two seasons, the summer frontal location at Cape Town, in turn, exhibits remarkable stability. The upwelling off Lüderitz, on the other hand, is prone to almost constant frontal location fluctuations.

Most of the variation occurs as a result of the growth and decay of filaments. Filaments were seen along the entire upwelling zone from Cape Agulhas to Cape Frio. On average, the filament sector was 270 kilometres wide off Lüderitz. Between Cape Point and Cape Agulhas the southwards extent of the upwelling rarely exceeded 40 kilometres, while the maximum filament off Cape Point was about 200 kilometres. As a rule, the Cape Point filament was about 40 kilometres long and the upwelling zone off Walker Bay 20 kilometres wide. Large scale reductions in the surface area of the upwelling resulting from the anomalously high sea temperatures of 1982/83 (Walker et al. 1984), clearly showed in the extracted satellite data. The images used were not calibrated to show actual sea surface temperature, however. Consequently, ships data were used to determine the cross-frontal temperature gradient.

With the extensive filament off Lüderitz during 1982 as an example, a frontal temperature gradient of between  $0.02^{\circ}\text{C}$  and  $.006^{\circ}\text{C}$  per kilometre was measured. This compares well with readings in the Californian upwelling zone (Koblinsky et al. 1984). How this compared with the situation in the southwestern Cape upwelling region was not calculated. With the differences in offshore water composition and the physical characteristics of the currents bounding the two southern African upwelling zones, it is unlikely that the frontal temperature gradients would be comparable. Common to both the Cape and Lüderitz upwelling regions, however, is the swift response of the filaments to the passage of mesoscale weather systems.

The coastal low pressure systems and the associated berg winds were seen as prominent factors in filament growth and decay off Lüderitz. The growth of filament extent during

those berg winds able to transport dust offshore was noteworthy. In the southern study area bud-off high pressure systems and passing cyclonic lows respectively induced or suppressed upwelling (Jury 1985, Nelson 1985). The response of the upwelling front to the more general weather systems is somewhat different, however. At the capes the dominance of the South Atlantic Anticyclone induced winds in summer gave rise to the extremely stable upwelling there. At Lüderitz the picture is not as clear. Contrary to what one might expect after studying the work of Lutjeharms (1981a) on the influence of winds of the previous ten days upon sea surface temperature patterns, no relationship was found between the winds of the previous 10-days and the location of the upwelling boundaries. This result suggested alternative explanations were required to resolve the problem of what induces and sustains the filament growth at Lüderitz in comparison to that at Cape Town. A partial solution to the questions raised by this situation lies in the examination of the difference in the preferred tracks followed by filaments at both locations.

The orientation of the filament tracks found appears to implicate the macroscale bathymetry in the paths that the Lüderitz filaments follow as they stream into the South-East Atlantic Ocean. The extraordinary filament off Lüderitz during 1982 appeared to be sustained by an accelerated flow through a gap in the Walvis Ridge. Extensive filaments off Cape Frio appeared to follow the line of the Ridge (Lutjeharms and Stockton 1987). Thus, with respect to the fact that undersea topography playing an important part in their creation and morphology, cape filaments may be related to those off Lüderitz. In contrast, the cape filaments are a product of the nearshore bathymetry, while the bathymetric features seen as influencing the Lüderitz filament are some hundreds of kilometres offshore. This may well explain the ability of the deep-sea filaments to reach great lengths, while those off the capes rapidly dissipate during relatively short periods of unfavourable winds. In a sense the deep-sea filament is pulled from the coast by the accelerated flow through the gap in the Walvis Ridge, while the cape filament is pushed from the rear by the Bernoulli acceleration as it rounds the cape. This can be explained using the analogy of cooked spaghetti. A string of this foodstuff is more effectively stretched to its full length by being pulled along the plate. By pushing, one causes the soft spaghetti to crumple into a short, convoluted tangle. Another aspect in which both similarities and disparities are seen is in the reaction of the two upwelling zones to the wind fields.

Easterly winds are clearly influential in determining the nature of upwelling in both the study areas. The berg wind was a major driving force off Lüderitz, although it was not a requirement. This is clear when it is noted that in none of the images studied were there signs of upwelling not being active at Lüderitz. This was not so at the capes. In fact, it became clear that at the capes there was a threshold wind velocity or favourable wind duration required for upwelling to form at all. Thus there are periods where upwelling does not occur along the southern Cape coast at all. Consequently, a cycle of upwelling at the capes is possible.

The proposed cycle takes the form of three basic sea surface temperature patterns. Firstly, a situation arises after a period of winds unfavourable to cape upwelling where there is upwelling north of Cape Point, not between Cape Point and Cape Agulhas. The second part of the cycle starts after a short-period of upwelling favourable easterly winds, giving rise to upwelling filaments at all at the capes. Finally, should the easterly winds continue there is full extensive and contiguous upwelling along the whole coast between Cape Point and Cape Agulhas. Probably owing to the greater persistence in upwelling favourable winds along the Namib Desert coast no such cycle could be seen for the deep-sea filaments.

It is not implausible to suggest that there are cycles to the filament activity in the deep-sea filaments. This is an area that could be the topic of further research. Another endeavour that would also be worthwhile is the modelling of the frontal reaction to passing mesoscale weather systems. Nelson (1985) attempted this at a coarse scale. Satellite imagery of the kind used here would enable this exercise to be expanded upon with greater precision.

Therefore, while this work has added to the body of knowledge concerned with the important and ecological important frontal zone of the Benguela Upwelling system, it is clear that there is much that still needs to be done.

## REFERENCES

1. Allanson B.R., Hart R.C. and J.R.E. Lutjeharms, 1981 - Observtions on the nutrients, chlorophyll and primary production of the Southern Ocean south of Africa. S. Afr. J. Antact. Res., 10/11: 3 - 14.
2. Andrews W.R.H. and L. Hutchings, 1980 - Upwelling in the Southern Benguela Current. Prog. Oceanogr., 9(1): 81 pp.
3. Bang N.D. ,1971 - The Southern Benguela Current Region in February 1966; Bathythermography and air-sea interactions. Deep-Sea Res., 18 (2): 209 - 255.
4. Bang N.D. and W.R.H. Andrews, 1974 - Direct current measurements of a shelf-edge frontal jet in the southern Benguela system. Jnl mar. Res., 32(3): 405 - 417.
5. Bernstein R.L., Breaker L. and R. Whritner, 1977 - California eddy formation : ship, air and satellite results. Science, New York, 195(4276): 353 - 359.
6. Boyd A.J., Tromp B.B.S. and D.A. Horstman, 1985 - The Hydrology off the South African south-western coast between Cape Point and Danger Point in 1975. S. Afr. J. mar. Sci., 3: 145 - 168.
7. Brink K.H., 1983 - The near-surface dynamics of coastal upwelling. Prog. Oceanogr., 12(3): 223 - 257.
8. Brink K.H.,1987 - Upwelling fronts: implications and unknowns. The Benguela and Comparable Ecosystems, A.I.L. Payne, Gulland, J.A. and K.H. Brink (Eds). S. Afr. J. mar. Sci., 5: 3 - 11.
9. Catzel R. and J.R.E. Lutjeharms, 1987 - Agulhas Current border phenomena along the Agulhas Bank south of Africa. CSIR Research Report, 635: 1 - 22.
10. Copenhagen W.J., 1953 - The periodic mortality of fish in the Walvis region; a phenomenon within the Benguela Current. Investl Rep. Div. Fish. S. Afr., 14: 35 pp.
11. Currie R., 1953 - Upwelling in the Benguela Current. Nature, Lond., 171(4351): 497 - 500.
12. Darbyshire M., 1966 - The surface waters near the coasts of Southern Africa. Deep-Sea Res., 13(1): 57 - 81.
13. Dengler A.T., 1985 - Relationship between physical and biological processes at upwelling fronts of Peru, 15 S. Deep-Sea Res., 32(114): 1301 - 1315.
14. Feldman G.C., 1986 - Variability of the productive habitat in the Eastern Equatorial Pacific. Trans. Am. geophys. Un., 67(9): 106 - 108.
15. Flament P., 1988 - Mixed-layer fronts in the California Current. Internal Report, Woods Hole Oceanographic Institution, Woods Hole, Massachusetts.
16. Flament P., Armi L. and L. Washburn, 1985 - The evolving structure of an upwelling Filament, J. geophys. Res., 90(C6): 11765 - 11778.

17. Gordon H.R., Clark D.K., Brown J.W., Brown O.B. and R.H. Evans, 1982 - Satellite measurement of phytoplankton pigment concentration in the surface waters of a warm core Gulf Stream ring. J. mar. Res., 40(2):491 - 502.
18. Harris T.F.W. and L.V. Shannon, 1979 - Satellite tracked drifter bouys in the Benguela Current System. S. Afr. J. Sci., 75(7): 316 - 317.
19. Hart T.J. and R.I. Currie, 1960 - The Benguela Current. "Discovery" Rep., 31: 123 - 298.
20. Jackson S.P., 1951 - Climates of Southern Africa. S. Afr. J. Sci., 31: 17 - 37.
21. Jury M.R., 1985 - Case Studies of Alongshore Variations in Wind-driven Upwelling in the Southern Benguela Region. South African Ocean Colour and Upwelling Experiment, Shannon, L.V. (Ed.), Cape Town; Sea Fisheries Research Institute, pp. 29 - 46.
22. Jury M.R., 1988 - A climatological mechanism for wind-driven upwelling near Walker Bay and Danger Point, South Africa. S. Afr. J. mar. Sci., 6: 175 - 181.
23. Jury M.R., Kamstra F. and J. Taunton-Clark, 1985 - Synoptic summer wind cycles and upwelling off the southern portion of the Cape Peninsula. S. Afr. J. mar. Sci., 3: 33 - 42.
24. Kamstra F., 1985 - Environmental features of the Southern Benguela with special reference to wind stress. South African Ocean Colour and Upwelling Experiment, Shannon L.V. (Ed.), Cape Town, Sea Fisheries Research Institute, pp. 13 - 27.
25. Koblinsky C.J., Simpson J.J. and T.D. Dickey, 1984 - An offshore eddy in the California Current system. Prog. Oceanogr., 13(1): 1 - 71.
26. Kosro P.M. and A. Huyer, 1985 - CTD and DAL surveys of seaward jets off northern California, July 1981 and 1982. Trans. Am. geophys. Un., 66(51): 1258.
27. Lutjeharms J.R.E., 1981a - Satellite studies of the South Atlantic upwelling system. In: Oceanography from Space, J.F.R. Gower (Ed.), Plenum Press, New York, pp. 195 - 199 (Marine Science, 13).
28. Lutjeharms J.R.E., 1981b - Features of the southern Agulhas Current circulation from satellite remote sensing. S. Afr. J. Sci., 77(5): 231 - 236.
29. Lutjeharms J.R.E. and H.R. Valentine, 1987 - Water types and volumetric considerations of the South East Atlantic upwelling regime. The Benguela and Comparable Ecosystems, A.I.L. Payne, Gulland, J.A. and K.H. Brink (Eds). S. Afr. J. mar. Sci., 5: 63 - 71.
30. Lutjeharms J.R.E and J.M. Meeuwis, 1987 - The Extent and Variability of South-East Atlantic Upwelling. The Benguela and Comparable Ecosystems, A.I.L. Payne, Gulland, J.A. and K.H. Brink (Eds). S. Afr. J. mar. Sci., 5: 51 - 62.
31. Lutjeharms J.R.E and P.L. Stockton, 1987 - Kinematics of the upwelling front off Southern Africa. The Benguela and Comparable Ecosystems, A.I.L. Payne, Gulland, J.A. and K.H. Brink (Eds). S. Afr. J. mar. Sci., 5: 35 - 49.

32. Lutjeharms J.R.E., Walters N.M., and B.R. Allanson, 1985 - Oceanic frontal systems and biological enhancement. Antarctic Nutrient Cycles and Food Webs, Siegfried W.R., Condy P.R. and R.M. Laws (Eds). Berlin; Springer, pp. 11 - 21.
33. Marra J., Houghton R.W., Boardman D.C., and P.J. Neale, 1982 - Variability in surface chlorophyll at a shelf break front. J. mar. Res., 40(3): 575 - 591.
34. Mooers C.N.K. and A.R. Robinson, 1984 - Turbulent jets and eddies in the Californian Current and inferred cross-shore transports. Science, New York, 223(4631): 51 - 53.
35. Moroshkin K.V., Bubnov V.A. and R.P. Bulatov, 1970 - Water circulation in the eastern South Atlantic Ocean. Oceanology, 10(1): 27 -34.
36. Nelson G., 1985 - Notes on the physical oceanography of the Cape Peninsula Upwelling. South African Ocean Colour and Upwelling Experiment, Shannon L.V. (Ed.), Cape Town, Sea Fisheries Research Institute, pp. 63 - 95.
37. Nelson G. and A. Polito, 1987 - Information on currents in the Cape Peninsula area, South Africa. The Benguela and Comparable Ecosystems, A.I.L. Payne, Gulland, J.A. and K.H. Brink (Eds). S. Afr. J. mar. Sci., 5: 275 - 304.
38. Nelson G. and L. Hutchings, 1983 - The Benguela upwelling area. Prog. Oceanogr., 12: 333 - 359.
39. Olson D.B. and R.H. Backus, 1985 - The concentrating of organisms at fronts: cold-water fish and a warm core Gulf Stream ring. J. mar. Res., 43(1): 113 - 137.
40. Olson D.B. and R.H. Evans, 1986 - Rings in the Agulhas Current. Deep-Sea Res., 33(1): 27 - 42.
41. Parrish R.H., Bakun A., Husby D.M. and C.S. Nelson, 1983 - Comparative climatology of selected environmental processes in relation to eastern boundary current pelagic fish production. Proc. Expert consultation to examine changes in abundance and species composition of neritic fish stocks, Sharp G.D. and J. Csirke (Eds)., San Jose, Costa Rica, FAO Fish Rep., 291(3): 731 - 777.
42. Perry A.H and J.M. Walker, 1977 - The Ocean-Atmosphere System, Longman, New York, pp. 50 - 128.
43. Pingree R.D., Mardell G.T., Holligan P.M., Griffiths D.K. and J. Smithers, 1982 - Celtic Sea and Armorican Current structure and the vertical distribution of temperature and chlorophyll. Continental Shelf Res., 1(1): 99 - 116.
44. Planke J., 1977 - Phytoplankton biomass and productivity in the Subtropical Convergence area and shelves of the western Indian subantarctic islands. Adaptions within Antarctic Ecosystems, Llano G.A.(Ed.). Houston; Gulf Publishing Company, pp. 51 - 73
45. Schell I.I., 1970 - Variability and Persistence in the Benguela Current and Upwelling off Southwest Africa. J. geophys. Res., 75(27): 5225-5241.

46. Schulze, B.R., 1974 - Climate of South Africa, Part 8, General Survey. South African Weather Bureau. Dept Environmental Affairs, Pretoria.
47. Schumann E.H., Perrins L.-A. and I.T. Hunter, 1982 - Upwelling along the South Coast of the Cape Province, South Africa. S. Afr. J. Sci., 78(6): 238 - 242.
48. Shannon L.V., 1985 - The Benguela Ecosystem : Part I. Evolution of the Benguela, Physical Features and Processes. In Oceanography and Marine Biology. An Annual Review, 23. Barnes, M (Ed.).Aberdeen University Press: 105 - 182.
49. Shannon L.V., 1986 - The Benguela Ecosystem, Part III. Plankton, In Oceanography and Marine Biology. An Annual Review, 24. Barnes, M (Ed.).Aberdeen University Press: 65 - 170.
50. Shannon L.V. Walters N.M. and Mostert S.A., 1985 - Satellite Observations of Surface Temperature and Near-Surface chlorophyll in the Southern Benguela. South African Ocean Colour and Upwelling Experiment, Shannon, L.V. (Ed.),Cape Town; Sea Fisheries Research Institute, pp. 183 - 210.
51. Shannon L.V., Agenbag J.J. and M.E.L. Buys, 1987 - Large- and mesoscale features of the Angola-Benguela front. The Benguela and Comparable Ecosystems, A.I.L. Payne, Gulland, J.A. and K.H. Brink (Eds). S. Afr. J. mar. Sci., 5: 11 - 34.
52. Shannon L.V., Nelson G. and M. Jury, 1981 - Hydrology and meteorological aspects of upwelling in the southern Benguela current. in Coastal and Estuarine Sciences 1. Coastal Upwelling, Richards F.A. (Ed.) Washington D.C., American Geophysical Union, pp. 146-159.
53. Simpson J.H., Edelstein D.J., Edwards A., Morris N.C.G. and P.B. Tett, 1979 - The Islay front:physical structure and phytoplankton distribution. Estuar. coast. mar. Sci., 9(6): 713 - 726.
54. Stockton P.L. and J.R.E. Lutjeharms, 1988 - Observations of vortex dipoles on the Benguela upwelling front. S.Afr. Geogr., 15 (1 & 2): 27 - 36.
55. Taljaard J.J., 1972 - Synoptic meteorology of southern Africa. Meteorology of the Southern Hemisphere, C W Newton (Ed.), Boston; American Meteorological Society, Meteorological Monographs, 13(5), pp. 139 - 213.
56. Taunton-Clark J., 1985 - The formation, growth and decay of upwelling tongues in response to the mesoscale wind field during summer. South African Ocean Colour and Upwelling Experiment, Shannon L.V. (Ed.), Cape Town, Sea Fisheries Research Institute, pp. 47 - 62.
57. Van Foreest D., Shillington F.A. and R. Legeckis, 1984 - Large scale, stationary frontal features in the Benguela Current system. Continent. Shelf Res., 3(4): 465 - 474.
58. Walker N.D., Taunton-Clark J. and J. Pugh, 1984 - Sea temperatures off the South African West Coast as indicators of Benguela Warm Events, S. Afr. J. Sci., 80(2): 72 - 77.

59. Yentsch C.S. and D.A. Phinney, 1985 - Rotary motions and convection as a means of regulating primary production in warm core rings. J. geophys Res., 90(C2): 3237 - 3248.

## APPENDIX 1

Papers and publications arising out of the research towards the compilation of this thesis.

## PUBLICATIONS

- Lutjeharms J.R.E and P.L. Stockton, 1987 - Kinematics of the upwelling front off Southern Africa. The Benguela and Comparable Ecosystems, A.I.L. Payne, Gulland, J.A. and K.H. Brink (Eds). S. Afr. J. mar. Sci., 5: 35 - 49.
- Olivier J. and P.L. Stockton, 1988 - The influence of upwelling extent of advective fog occurrence at Lüderitz, southern Africa. Jnl Clim. (in press)
- Stockton P.L. and J.R.E. Lutjeharms, 1988 - Observations of vortex dipoles on the Benguela upwelling front. S.Afr. Geogr., 15 (1 & 2): 27 - 36.
- Stockton P.L. and J.R.E Lutjeharms, 1988 - Aspects of the upwelling between Cape Point and Cape Agulhas. S. Afr. J. mar. Sci., (submitted).

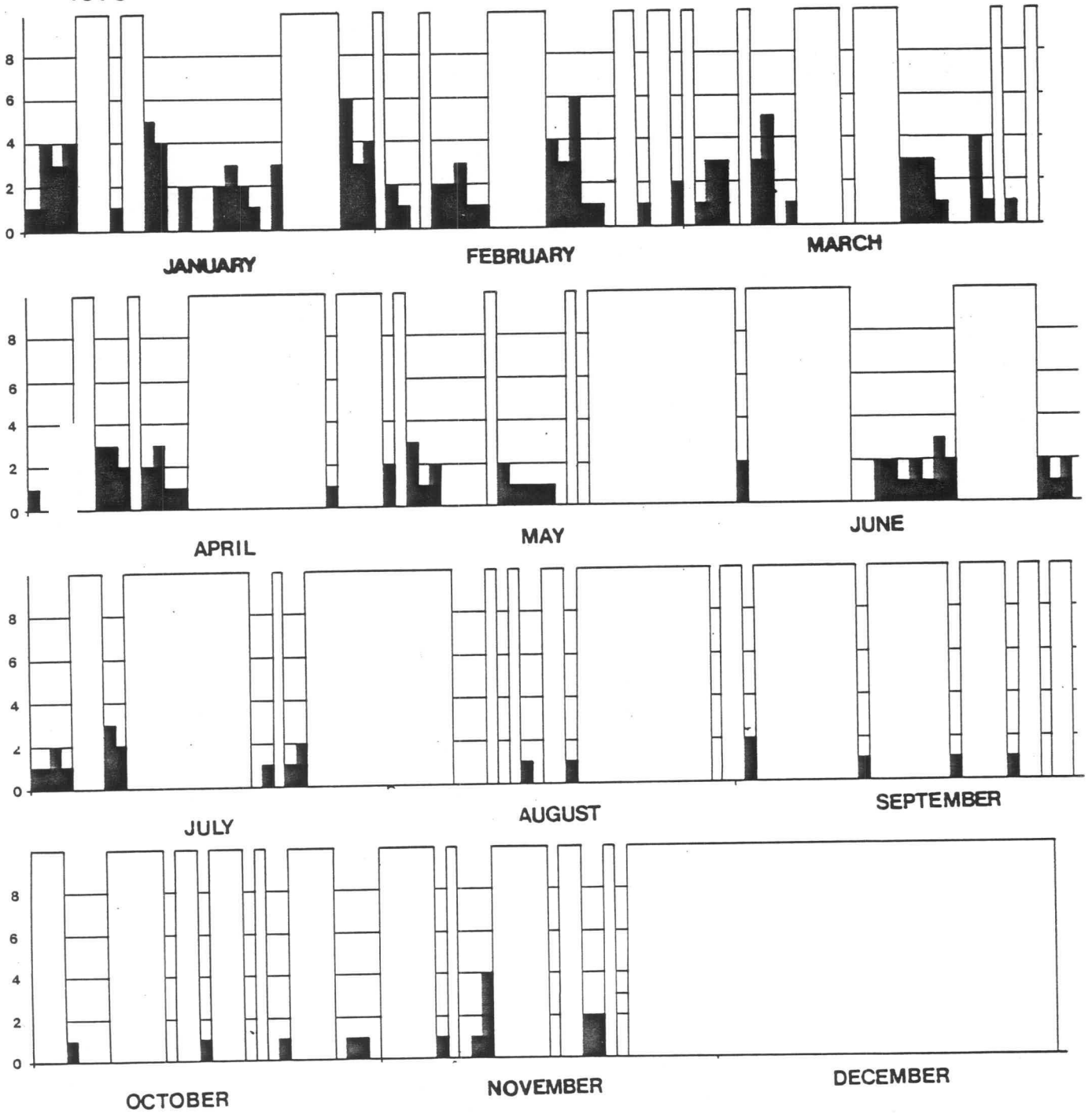
## PAPERS

- Lutjeharms J.R.E., P.L. Stockton and L.V. Shannon, 1986 - Kinematics of the upwelling front off southern Africa, Population and Community Ecology in the Benguela Upwelling Region and Comparable Frontal Systems, 8 - 12 September, University of Cape Town.
- Olivier J. and P.L. Stockton, 1987 - The influence of upwelling extent on fog formation at Luderitz, The Quadrennial Geographical Society Conference, University of Grahamstown.
- Stockton P.L. and J.R.E. Lutjeharms, 1987 - An exceptional upwelling filament off Lüderitz during 1982. 6th National Oceanographic Symposium, 6 - 10 July, University of Stellenbosch.
- Stockton P.L., 1987 - Thermal Boundaries of the Southern African west coast upwelling zone, National Conference on Long-Term Data Series Relating to Southern Africa's Natural Resources, 12 - 14 October, Pretoria.
- Stockton P.L. and J.R.E Lutjeharms, 1987 - Upwelling in the Walker Bay area. Benguela Ecology Project weekly seminar series, Department of Oceanography, University of Cape Town, 9 November, Cape Town.
- Stockton P.L. and J.R.E. Lutjeharms, 1988 - The Influence of Berg Winds on Upwelling at Lüderitz, Southern Africa. South African Society for Atmospheric Sciences Fifth Annual Conference, 17 - 19 October, Pretoria.

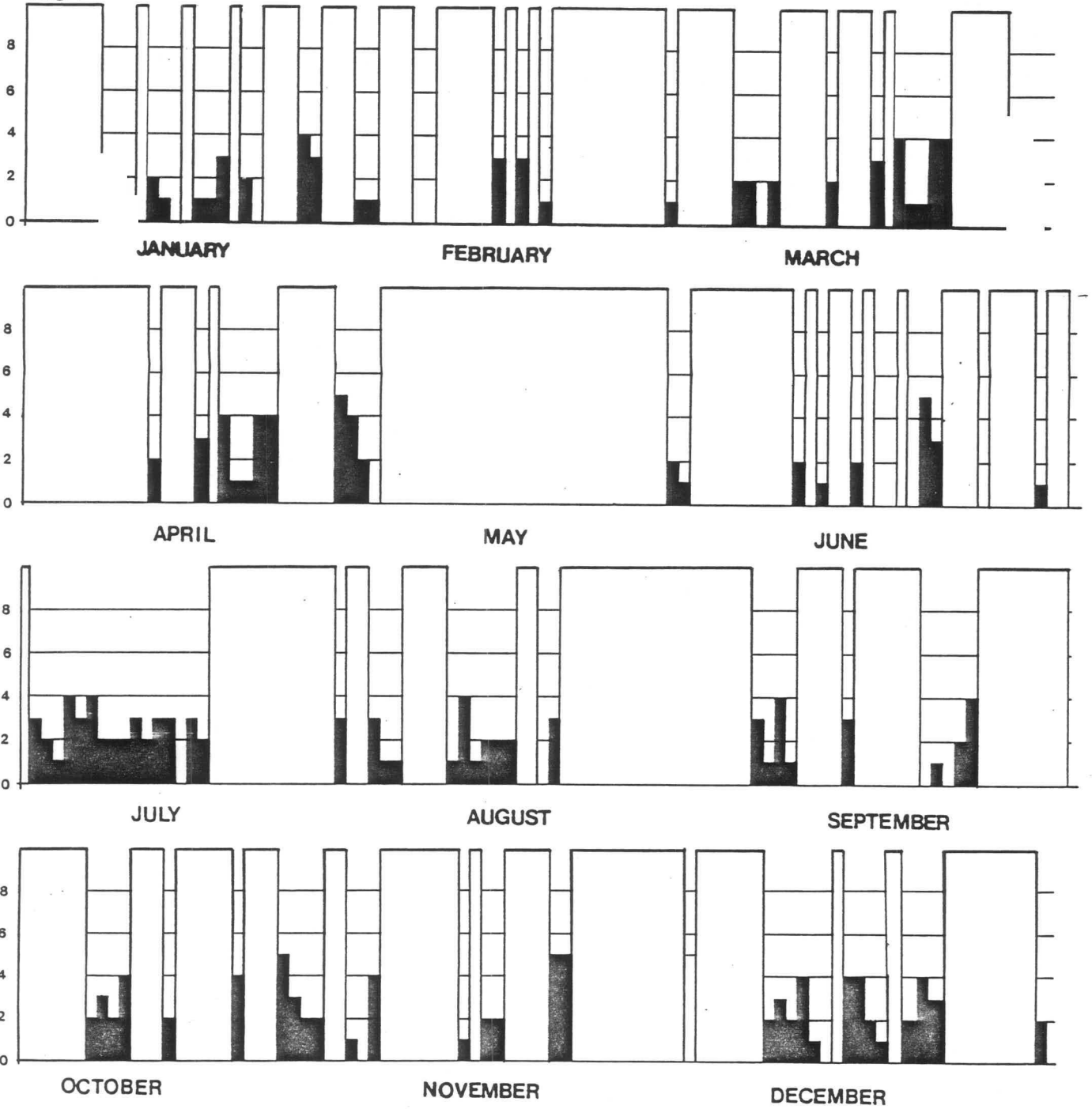
**APPENDIX 2**

Daily filament frequencies at Lüderitz between 1979 and 1985. The dark bars show the filament frequency, while the white areas represent the times when the sea surface was not visible to the Meteosat II satellite.

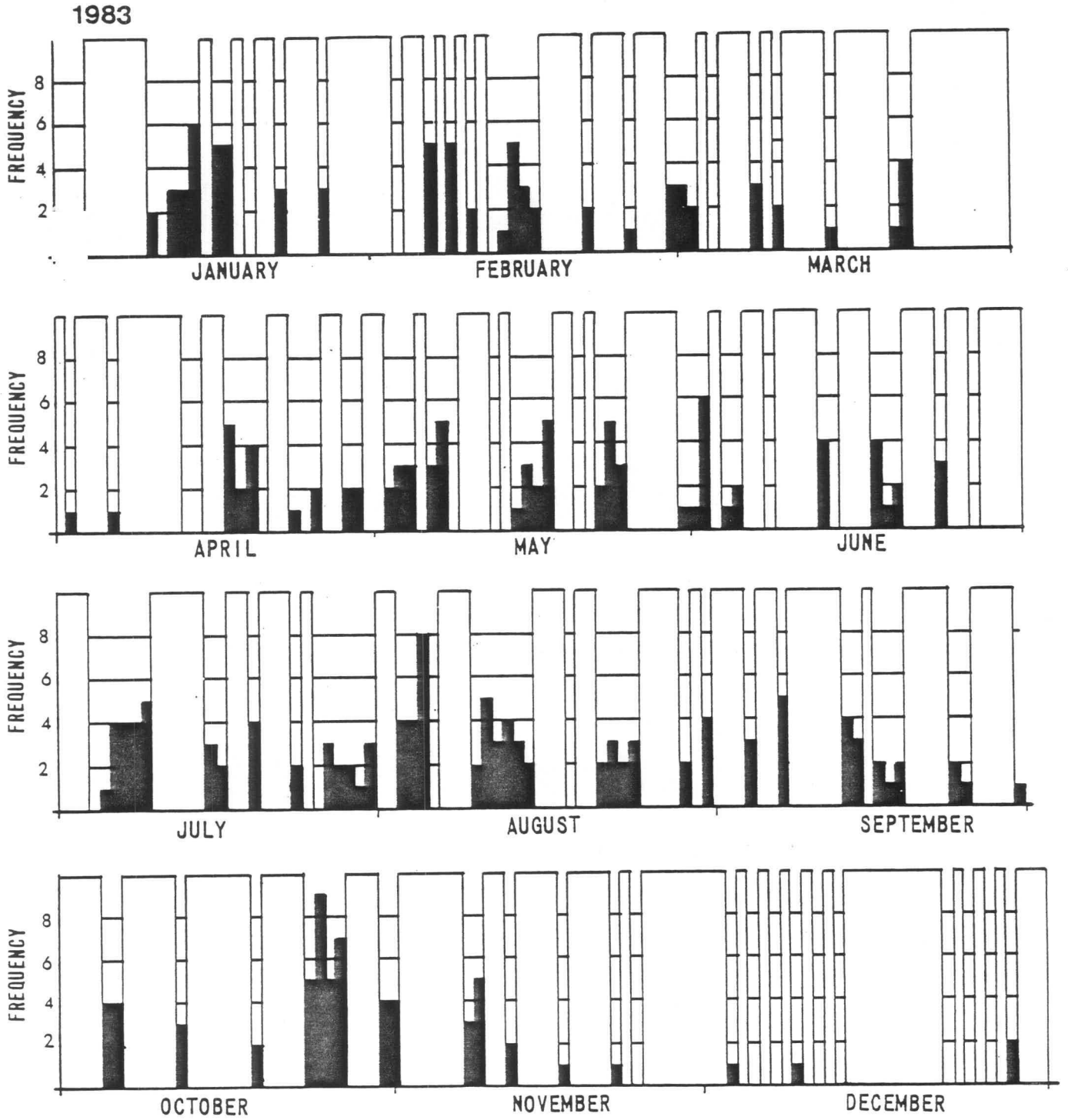
1979



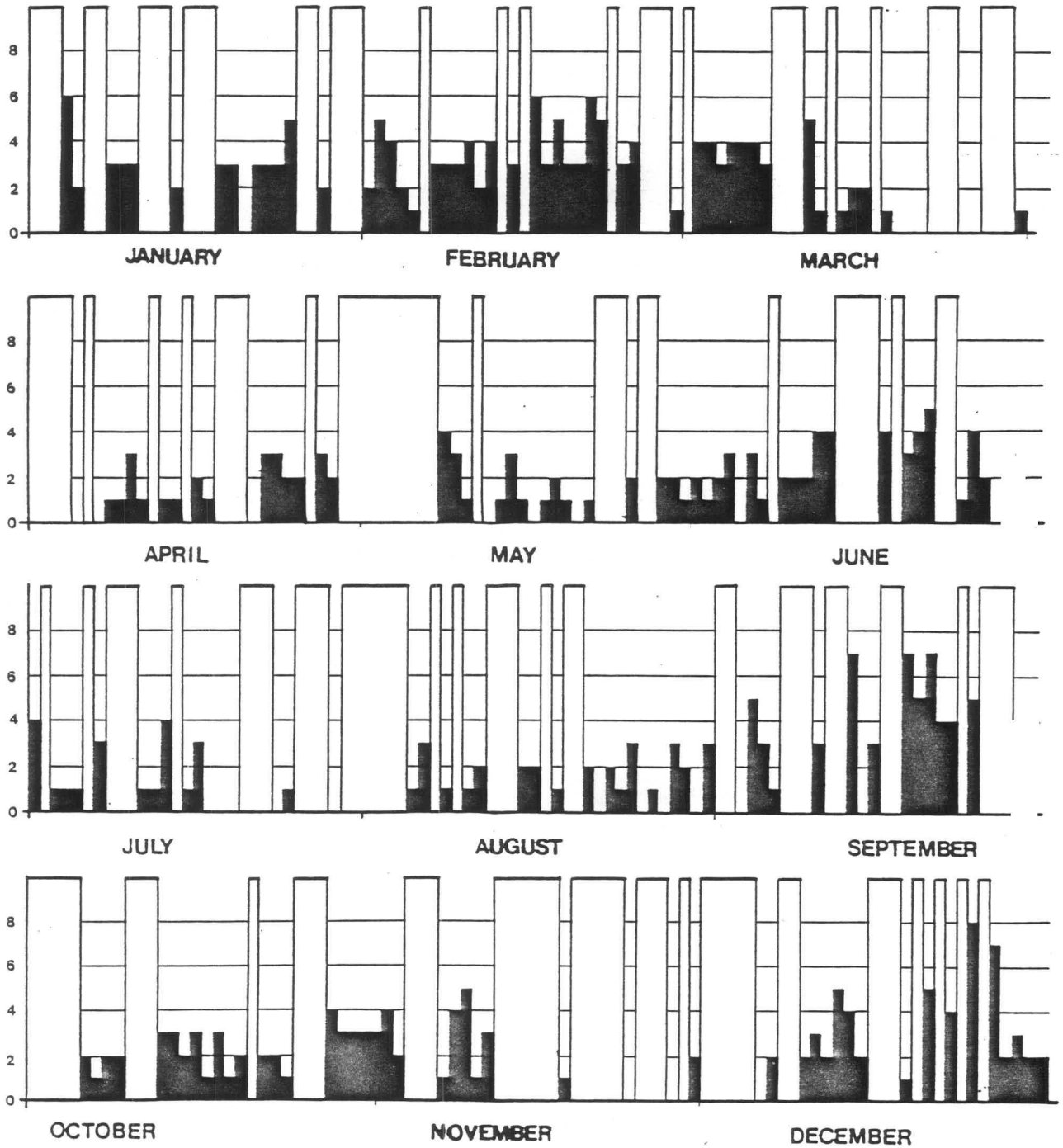
1982







1985

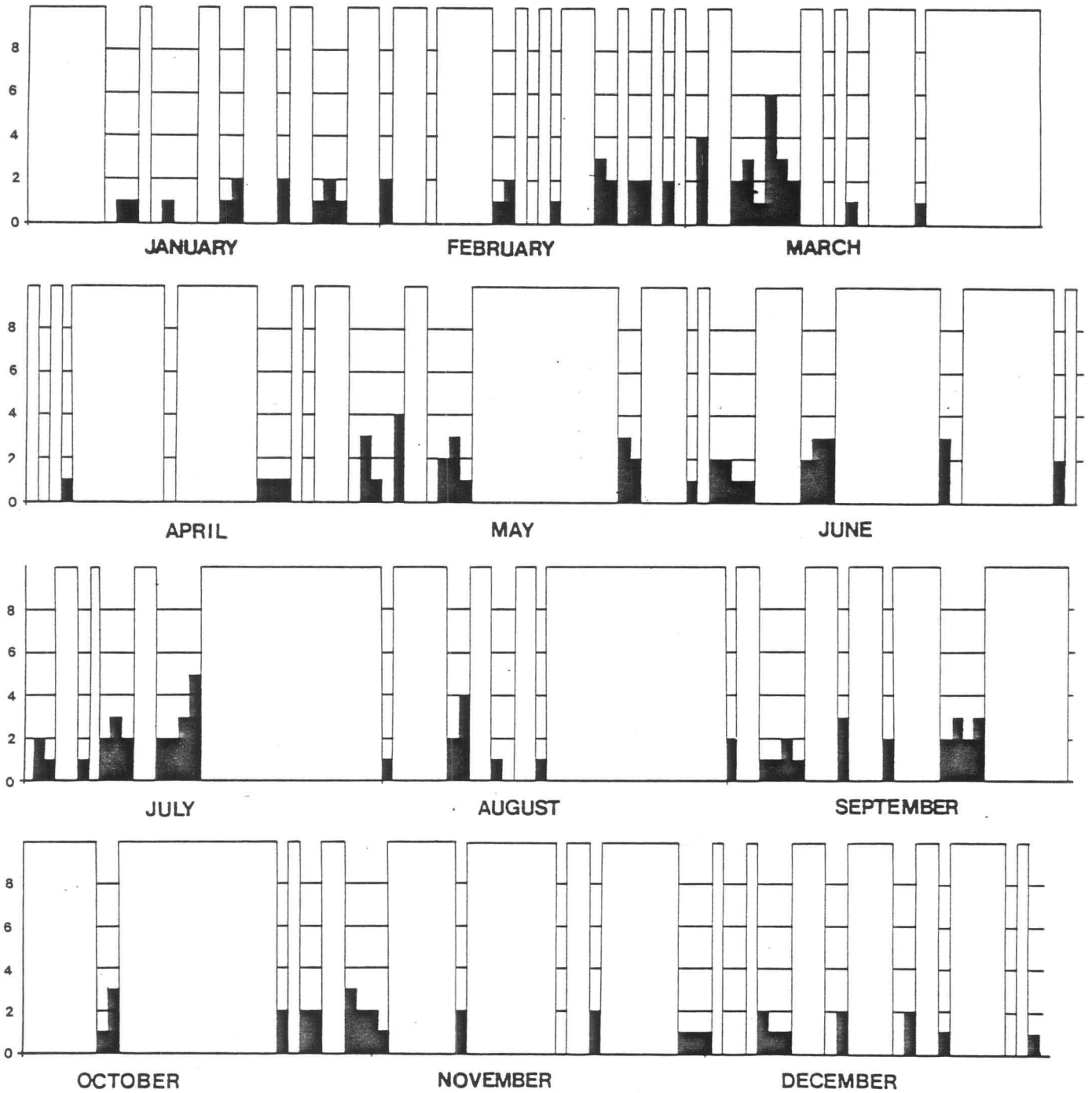


### APPENDIX 3

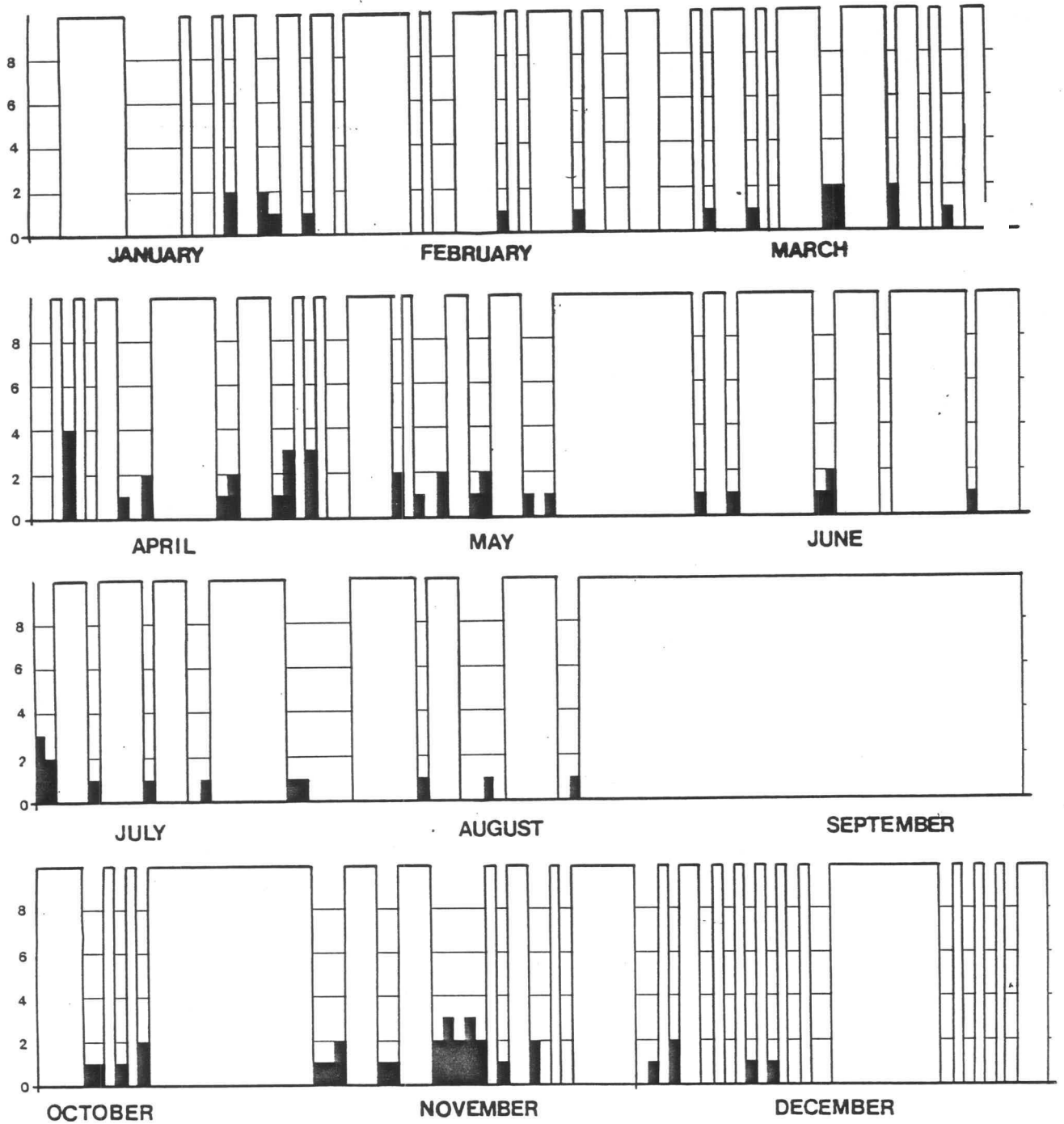
Daily filament frequencies at Cape Town between 1979 and 1985. The dark bars show the filament frequency, while the white areas represent the times when the sea surface was not visible to the Meteosat II satellite.



1982

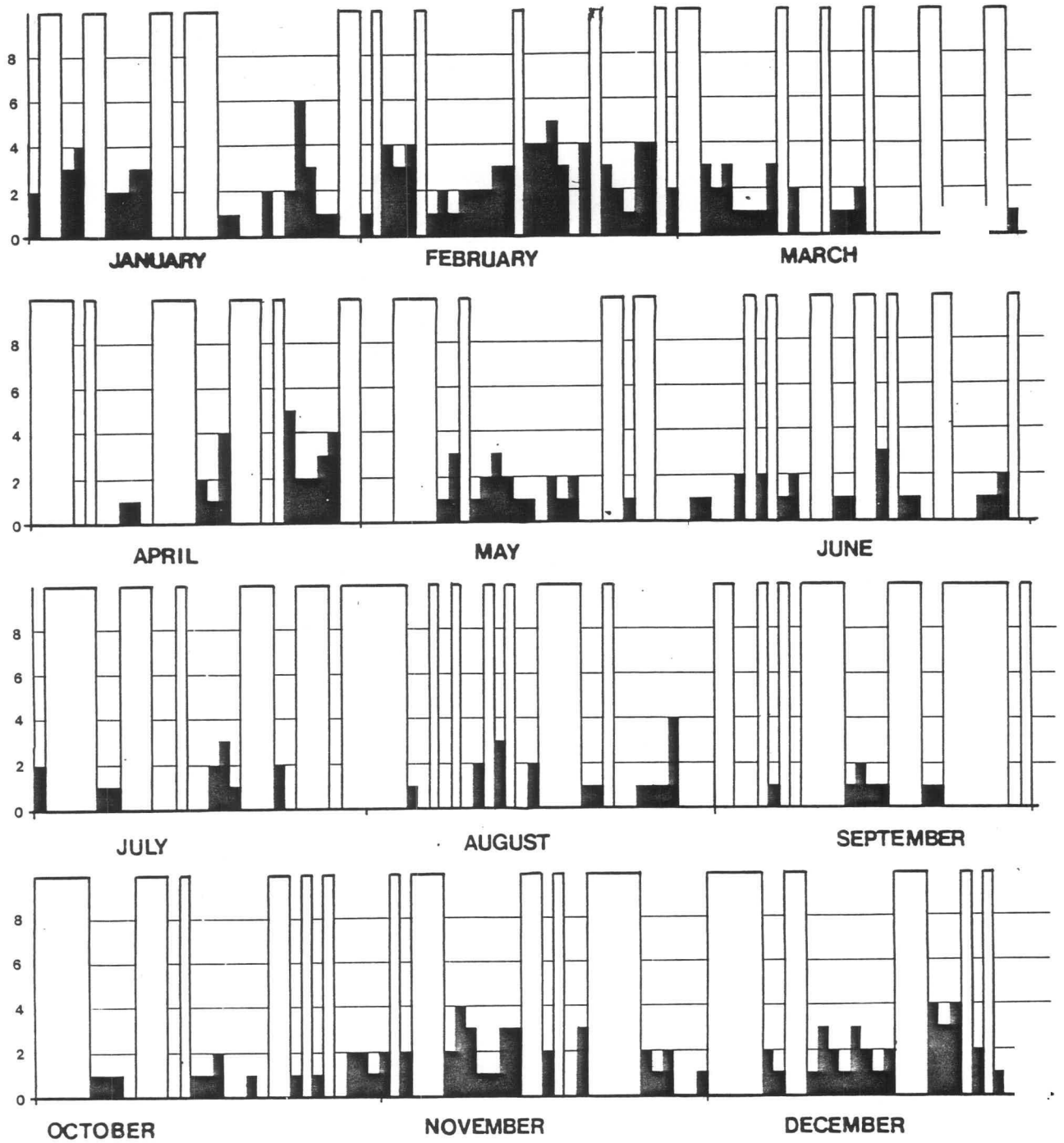


1983



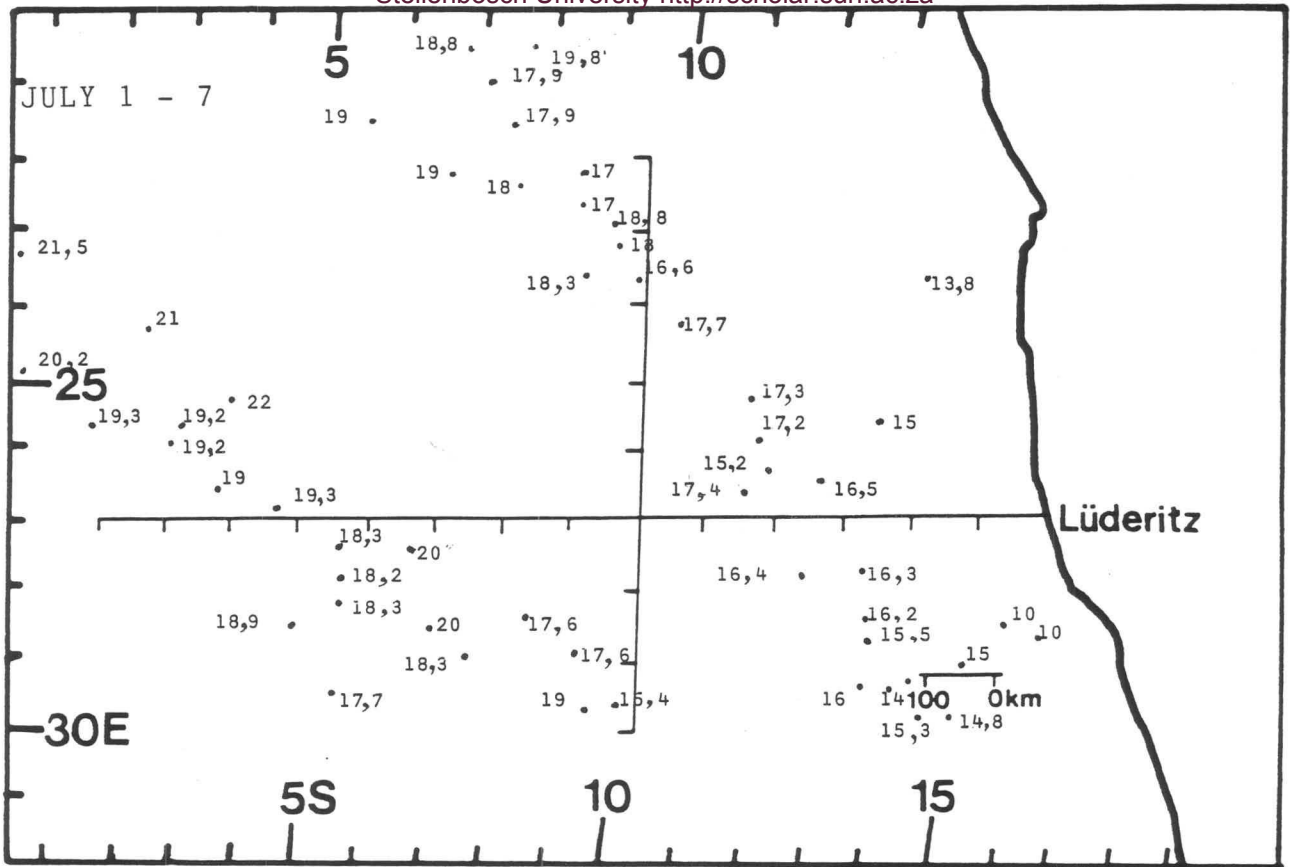


1985

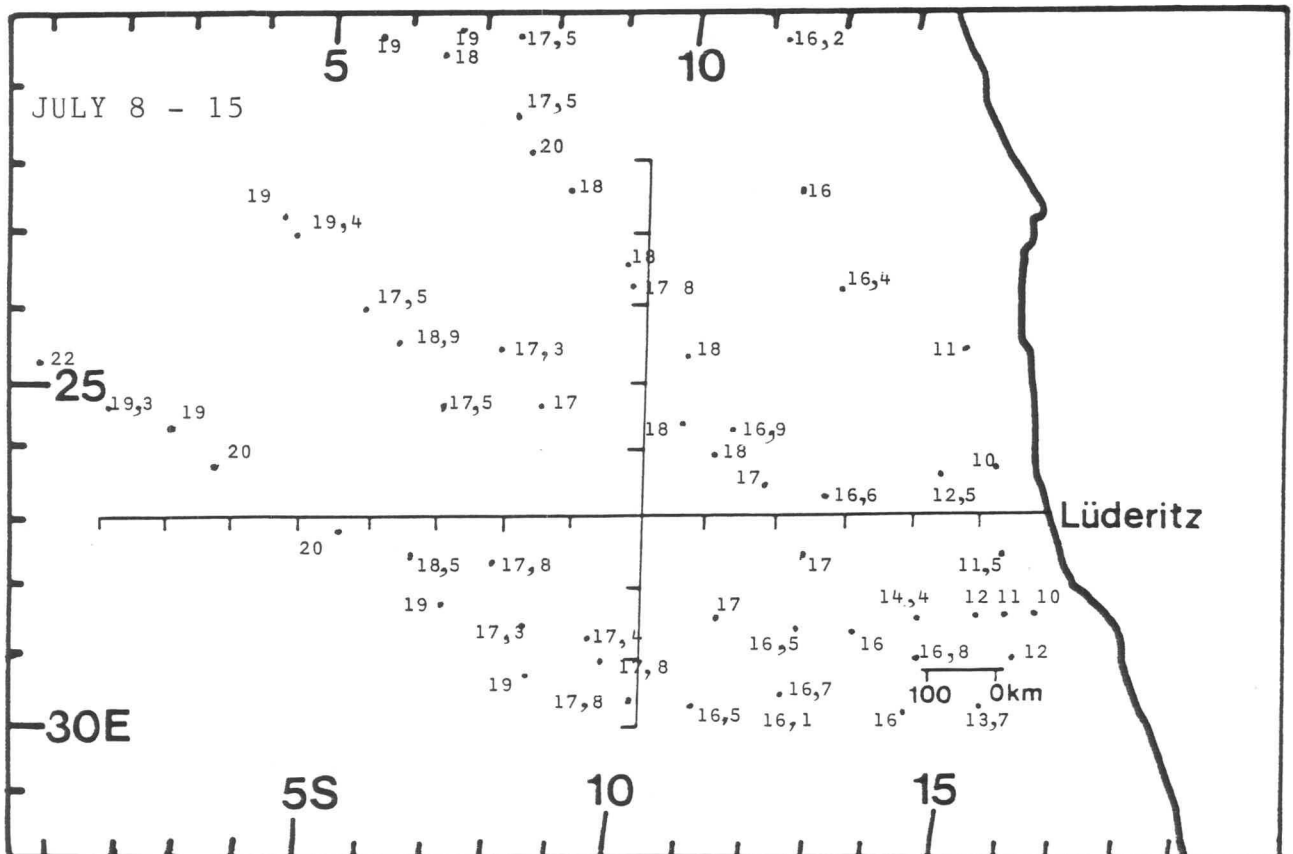


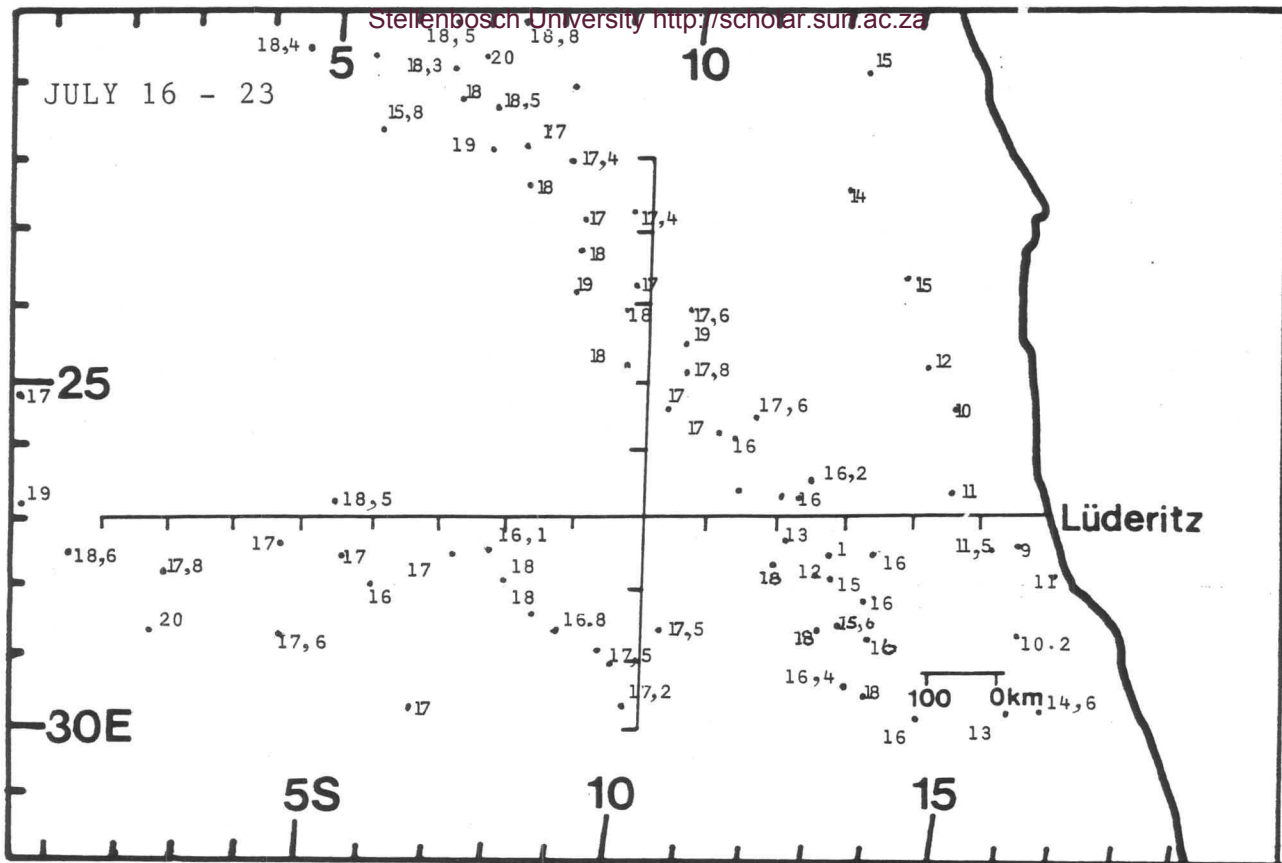
#### **APPENDIX 4**

The weekly sea surface temperature distribution as recorded by the merchant shipping during July, 1982. These data were used in the construction of Figure 3.5.



Sea surface temperatures as recorded by merchant shipping. These data were used to determine the sea surface contours shown in FIGURE 3.5.





Sea surface temperatures as recorded by merchant ships for the month of July, 1982. These data were used in the construction of the contour maps presented as FIGURE 3.5.

